Quantum Entanglement, Fidelity Susceptibility, and Scrambling from AdS/CFT correspondence

Yukawa Institute for Theoretical Physics, Kyoto University

Masamichi Miyaji

Abstract

In this thesis, I will study several phenomena and quantities which are related to quantum information theory, using AdS/CFT correspondence. AdS/CFT correspondence is the conjecture on the equivalence between quantum gravity and quantum field theory. I will first study fidelity susceptibility, which measures distance between quantum states, using AdS/CFT correspondence. I will propose a holographic dual of fidelity susceptibility, as volume of maximal volume time slice, extended into AdS. Then I will use fidelity susceptibility to study the phenomenon called scrambling. Scrambling denotes the status that initial excitation is completely mixed with the environment. I will show that the particular fidelity susceptibility can capture scrambling, and describe how this picture is consistent with the proposed holographic dual of fidelity susceptibility. Finally, I will consider non local operation in both CFT and gravity. Such operation corresponds to changing entanglement structure. And I will study how the entanglement structure is changed, and how averaged null energy condition is violated by those operations.

Contents

1 Introduction

Despite of decades of efforts by numerous researchers, nature of quantum gravity has remained yet unrevealed. This is mainly because general relativity is not renormalizable, which implies that it is necessary to fix infinite number of parameters in the effective action in order to construct a consistent theory. Such procedure is difficult to handle theoretically and experimentally. Since the effective action may contain infinite number of parameters, it requires infinite amount of effort to determine UV theory of quantum gravity from experiments, if there were no top-down constraints on the underlying UV theory.

String theory is such a candidate theory that realizes UV completion of general relativity[1][2]. In string theory, fundamental elements are not point particles but strings and branes, which moderate UV behavior of the theory beyond string scale, freeing theory from UV divergence at least at perturbative level. Beyond perturbation theory, there are several observations that supports that sting theory is a consistent theory of quantum gravity. One fact is that string theory can explain Bekenstein-Hawking formula[3][4] of black hole entropy[5],

$$S_A = \frac{A}{4G_N} \tag{1}$$

where A stands for the area of black hole horizon, and G_N is Newton constant. Bekenstein-Hawking formula was originally motivated by analogy between second law of thermodynamics and area theorem of black hole. However, because black hole does not have microscopic structure classically (called no hair theorem), large entropy of black hole has been a big mystery in general relativity since then. It was surprising and became a strong support of string theory, that string theory can indeed explain the origin of non trivial black hole entropy.

Another evidence that supports string theory is that consistent unitary quantum gravity should contain infinite tower of massive particles, which is typical characteristic of string theory[8]. This implies that string-like theory is inevitable, as long as one sticks to causal unitary quantum theory which can be described by effective action. These facts motivate us to study string theory in more detail.

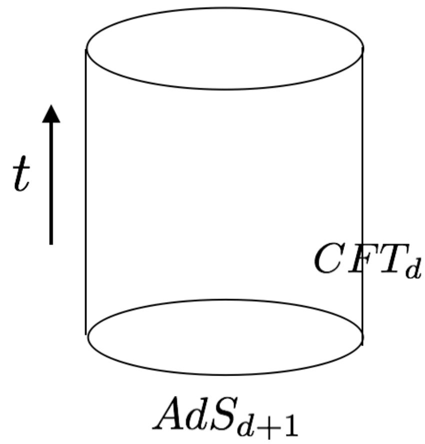

Figure 1: Interior of the cylinder corresponds to AdS_{d+1}, and the boundary, which is the cylinder, is where the CFT_d lives. AdS/CFT predicts that they are identical.

However, detailed non-perturbative properties of string theory is still hard to study, and up to now we know little beyond perturbative quantities or highly protected quantities. In order to go beyond, it is useful to consider holography, which conjectures that gravity can be described by the degrees of freedom at the boundary of the spacetime[6][7].

Holography or holographic principle is motivated by Bekenstein-Hawking formula of black hole entropy. Since G_N has dimension (length)$^{d-1}$ in $d+1$ dimensional spacetime, one can define a length scale

$$l_P := (4G_N)^{\frac{1}{d-1}}, \tag{2}$$

which is called Planck length. This length scale corresponds to that of the quantum gravity. Using Planck length, Bekenstein-Hawking formula can be interpreted as the statement, that order 1 degrees of freedom of black hole are contained in unit Planck area of black hole event horizon.

AdS/CFT correspondence is the most tested, concrete realization of holography[9][10][11]. AdS/CFT correspondence predicts that string theory on Anti de Sitter space (AdS) is equivalent to a conformal field theory on the boundary of AdS. AdS space is the Einstein manifold with constant negative scalar curvature, which is a vacuum solution of Einstein equation with negative cosmological constant. In Poincare coordinate, $d+1$ dimensional AdS is given by

$$ds^2 = R_{AdS}^2 \frac{dz^2 - dt^2 + \sum_{1\leq i\leq d-1} dx^i dx^i}{z^2} \tag{3}$$

where $z > 0$ and $z = 0$ corresponds to the boundary of AdS which is d dimensional Minkowski space, and R is AdS radius. In global coordinate, it is given by

$$ds^2 = R_{AdS}^2 \frac{1}{\cos^2\rho}(-dt^2 + d\rho^2 + \sin^2\rho \; d\Omega_{S^{d-1}}^2) \tag{4}$$

where $\rho > 0$ and $\rho = \pi/2$ corresponds to the boundary of AdS which is $R \times S^{d-1}$.

Let us assume $\phi(z,t,x)$ is a bulk real scalar field living on AdS, and the CFT action is deformed by external field $\int dtdx\phi_0(t,x)\mathcal{O}(t,x)$, where $\mathcal{O}(t,x)$ is real scalar primary operator. The precise statement of AdS/CFT in terms of partition function is called GKPW relation,

$$Z_{AdS_{d+1}}[\lim_{z\to 0} z^{-(d-\Delta)}\phi(z,t,x) \to \phi_0(t,x)] = Z_{CFT_d}[\int dtdx \; \phi_0(t,x)\mathcal{O}(t,x)] \tag{5}$$

where Δ is the conformal dimension of the primary operator. Although AdS/CFT correspondence has not been proven, it has proven to be valid in many concrete, non trivial examples.

Recent developments in AdS/CFT have revealed that quantum entanglement plays important role in AdS/CFT, therefore quantum gravity. The first achievement in this direction goes back to Bekenstein Hawking formula,

$$S_{BH} = \frac{A}{4G_N}, \tag{6}$$

which says the entropy of black hole S_{BH} is given by the area A of black hole event horizon. The generalization of Bekenestein Hawking entropy to entanglement entropy, called Ryu-Takayanagi (RT) formula[12], for subregion A of boundary timeslice dual to static asymptotically AdS spacetime (AAdS) is

$$S_A = \underset{\delta\Sigma=\delta A}{\text{Min}} \frac{\text{Area}[\Sigma]}{4G_N} \tag{7}$$

where Σ is codimension 2 surface in AAdS which is anchored from ∂A. We assume A and Σ are homologous to each other, meaning they can be identified with continuous deformations.

One can see that Ryu-Takayanagi formula satisfies correct properties of entanglement entropy, such as positivity, subadditivity, and strong subadditivity from simple geometric considerations[13]. It is known that Ryu-Takayanagi formula can be derived from AdS/CFT, using replica trick.

Importantly, Ryu-Takayanagi formula captures the equation of motion of gravity[15][16][17][18]. More precisely, let us consider first order perturbation of pure AdS spacetime, and assume that entanglement entropy of subregion A is given by the minimal value of the functional $F[\gamma]$ associated with a codimension 2 surface γ anchored from ∂A. $F[\gamma]$ depends only on fields on the surface γ. Once one assume $F[\gamma]$ is the area of γ, the assumption implies the linearized Einstein equation in the bulk. This fact implies that, the entanglement structure of the boundary CFT may be enough to capture the dynamics of gravity in the bulk, although

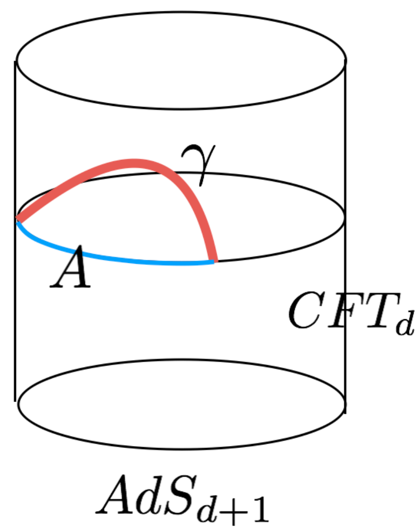

Figure 2: HRT surface in pure AdS. Black line at the cylinder corresponds to the timeslice of the CFT, and subregion A is expressed as blue line. Red curve γ is corresponding HRT surface.

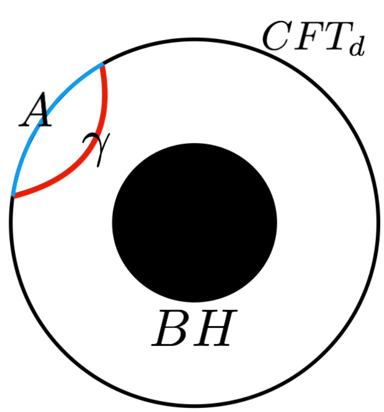

Figure 3: RT surface in BH geometry. This figure describes a timeslice of BH geometry. The boundary of the circle is the timeslice of CFT, and blue line is the subregion A. Red curve γ is the RT surface.

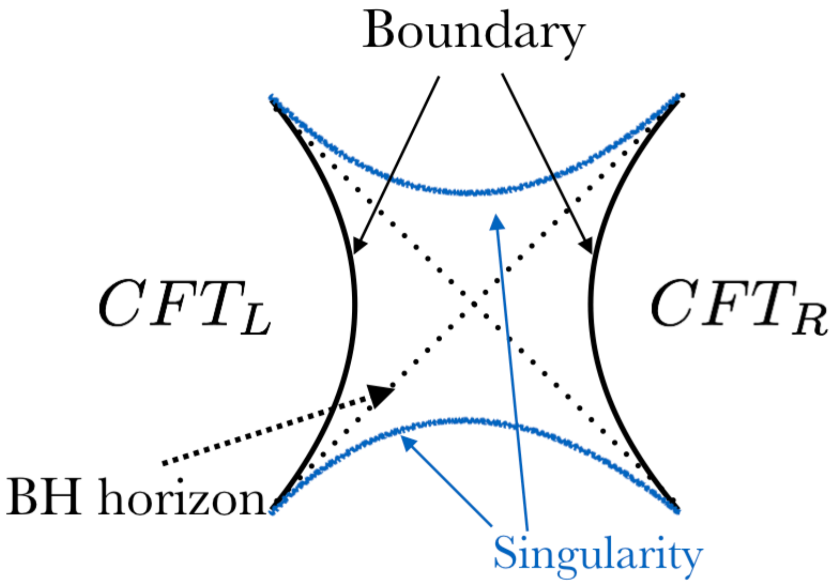

Figure 4: The geometry of two sided, asymptotically AdS black hole.

it is known that there are so called entanglement shadow where RT surface cannot probe, and also the argument only applies to linearized equation of motion.

There are also observations that imply spacetime connectedness comes from quantum entanglement[20]. Let us consider two sided asymptotically AdS black hole. The dual CFT is a tensor product $CFT_L \otimes CFT_R$, and dual CFT state is Thermofield double state[21],

$$|\Psi_{\text{TFD}}\rangle = \frac{1}{\sqrt{Z(\beta)}} \sum_i e^{-\frac{\beta E_i}{2}} |E_i\rangle_L \otimes |E_i\rangle_R, \tag{8}$$

where $\beta = \frac{1}{T}$ is the inverse temperature and $|E_i\rangle$s are eigenstates of the CFT Hamiltonian. The entanglement entropy between two CFTs is given by thermal entropy,

$$S_{CFT_L} = S_{CFT_R} = S_{therm}(\beta), \tag{9}$$

which approaches to zero when we take $\beta \to \infty$, and increases when we decrease β. The question is what happens to the geometry when we change quantum entanglement between two CFTs. The answer to this question is that, as one decreases the entanglement, the distance between two CFT increases, and when there are no entanglement, the two spacetimes are completely decoupled. This observation attempts us to interpret quantum entanglement is closely related to how the connectedness of the spacetime.

The generalization of Ryu-Takayanagi formula for time dependent situation is called Hubeny-Rangamani-Takayanagi (HRT) formula[19], which says

$$S_A = \underset{\delta\Sigma=\delta A}{\mathrm{Ext}} \frac{\mathrm{Area}[\Sigma]}{4G_N} \tag{10}$$

where Σ is codimension 2 surface in AAdS which is anchored from ∂A. We assume A and Σ are homologous to each other. In this time dependent extension, one can again prove inequalities of entanglement entropy, using so called max-min construction[22]. One starts with timeslice of bulk which contains A, and consider minimal surface anchored from ∂A which is contained in the time slice, then maximize that area by variating the timeslice. Then, it turned out that such max-min surface corresponds to HRT surface. Assuming null energy condition and Raychaudhri equation, one can prove inequalities such as strong subadditivity.

In this thesis, I will first review some basic facts about AdS/CFT correspondence and entanglement measures. Then I will propose a holographic dual of a quantum information theoretic measure, called fidelity susceptibility based on my paper[29]. Then I will propose an application of fidelity susceptibility to scrambling phenomena, and show how such application is related to dynamics of gravity in AdS/CFT based on my work [30]. Finally, I will consider non local operation in both CFT and gravity, which corresponds to changing entanglement structure using external operations based on my research [31].

2 AdS/CFT correspondence and Quantum Information Theory

In this section, I will review some basic facts about AdS/CFT correspondence and measures of quantum entanglement.

2.1 AdS/CFT correspondence

Let us first explain various coordinates of Anti de Sitter space. Anti de Sitter space can be considered as the universal cover of submanifold of flat space with metric

$$ds^2 = -(dX^0)^2 - (dX^{d+1})^2 + \sum_{1\le i\le d} (dX^i)^2, \tag{11}$$

with the condition

$$-(X^0)^2 - (X^{d+1})^2 + \sum_{1\le i\le d} (X^i)^2 = -R_{AdS}^2. \tag{12}$$

The global AdS is given by the relation

$$
\begin{aligned}
X^0 &= \sqrt{R_{AdS}^2+\rho^2}\sin(\frac{t}{R_{AdS}})\\
X^i &= \rho\ \Omega^i_{S^{d-1}}\\
X^{d+1} &= \sqrt{R_{AdS}^2+\rho^2}\cos(\frac{t}{R_{AdS}}),
\end{aligned}
\tag{13}
$$

where $\Omega_{1\le i\le d}$ denote the coordinate on $d-1$ dimensional sphere, so they satisfy

$$
\sum_{1\le i\le d}(\Omega^i_{S^{d-1}})^2 = 1.
\tag{14}
$$

Note that global AdS defines the universal cover of the manifold (12). In this language, Poincare patch is actually a submanifold of global AdS, and it is given by the condition

$$
\begin{aligned}
X^0 &= \frac{z}{2}(1+\frac{R_{AdS}^2+\sum_{1\le i\le d}x_i^2-t^2}{z^2})\\
X^i &= \frac{R_{AdS}x_i}{z}\\
X^d &= \frac{z}{2}(1-\frac{R_{AdS}^2-\sum_{1\le i\le d}x_i^2+t^2}{z^2})\\
X^{d+1} &= \frac{R_{AdS}t}{z}.
\end{aligned}
\tag{15}
$$

Let us consider another submanifold of global AdS, called Rindler-AdS. Rindler coordinate is given by

$$
\begin{aligned}
X^0 &= \xi\sinh(\frac{t}{R_{AdS}})\\
X^1 &= \xi\cosh(\frac{t}{R_{AdS}})\\
X^i &= \sqrt{R_{AdS}^2+\xi^2}\sinh(\frac{\eta}{R_{AdS}})\Omega^i_{S^{d-2}}\quad (i=2,\cdots,d)\\
X^{d+1} &= \sqrt{R_{AdS}^2+\xi^2}\cosh(\frac{\eta}{R_{AdS}})
\end{aligned}
\tag{16}
$$

with $\sum_i(\Omega^i_{S^{d-2}})^2=1$. Rindler-AdS is then given by

$$
ds^2 = -\frac{\xi^2}{R_{AdS}^2}dt^2+\frac{R_{AdS}^2}{R_{AdS}^2+\xi^2}d\eta^2+\frac{R_{AdS}^2+\xi^2}{R_{AdS}^2}\Big(d\xi^2+R_{AdS}^2\sinh^2(\frac{\eta}{R_{AdS}})d\Omega^2_{S^{d-2}}\Big).
\tag{17}
$$

These AdS spacetimes are called pure AdS, since they do not contain any excitations nor matter, and are indeed corresponding to vacuum state of gravity.

Once we consider excitations in both CFT and AdS, we need to consider asymptotically AdS spacetimes, with non trivial matter interior.

2.2 Entanglement Entropy and Entanglement Measures

In this section, I will review various measures of quantum entanglement that appear in quantum information theory [23].

2.2.1 Von Neumann Entropy

Here I list some basic but important properties of von Neumann entropy, for reference. Quantum state ρ is a Hermitian operator with nonnegative eigenvalues on Hilbert space with

$$\mathrm{Tr}[\rho] = 1. \tag{18}$$

And von Neumann entropy $S(\rho)$ of this state ρ, is given by

$$S(\rho) = -\mathrm{Tr}[\rho \mathrm{log} \rho]. \tag{19}$$

Von Neumann entropy is always non negative, and zero if and only if the state under consideration is pure. Also, von Neumann entropy is concave, meaning

$$\sum_i p_i S(\rho_i) \leq S(\sum_i p_i \rho_i) \tag{20}$$

for any $p_i \geq 0$ with $\sum_i p_i = 1$, and ρ_i are states. Von Neumann entropy is also additive, namely,

$$S(\rho_A \otimes \rho_B) = S(\rho_A) \otimes S(\rho_B) \tag{21}$$

holds.

2.2.2 Entanglement entropy

Let us assume Hilbert space of the whole system H can be decomposed into the tensor product of subsystem Hilbert space H and its compliment Hilbert space H_B, such that

$$H = H_A \otimes H_B. \tag{22}$$

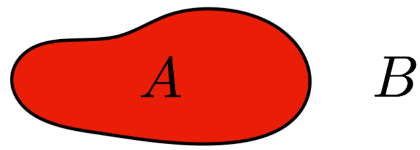

$$H = H_A \otimes H_B$$

Figure 5: Time slice is divided into two regions A and B. We assume corresponding Hilbert spaces factorizes. For QFT ground state, leading term of entanglement entropy of A is proportional to area of ∂A.

Then, for quantum state ρ on H, the quantum state on H_A

$$\rho_A := \mathrm{Tr}_{H_B}(\rho) \tag{23}$$

is the unique quantum state which can reproduce all the expectation values of operators living in H_A. Note that even if ρ is pure, ρ_A is not necessarily pure. The entropy of ρ_A is called entanglement entropy of the subsystem A, and it measures how the subsystem and its compliment are correlated to each other quantum mechanically as well as classically. Note that even if one starts with pure state which has no classical correlation, ρ_{sub} can be mixed state due to quantum correlation.

In quantum field theory, we often consider Hilbert space on subregion as a subsystem, and assume Hilbert spaces for the subregion and the compliment to be factorized. In general, entanglement entropy of subregion A, of the ground state of QFT in leading order is

$$S_A = c\frac{\mathrm{Area}[\partial A]}{\epsilon^{d-2}} + \cdots \ (d > 2) \tag{24}$$

$$S_A = \frac{c}{3}\log\frac{|A|}{\epsilon} \ (d = 2,\ \text{critical}) \tag{25}$$

$$S_A = c \cdot \mathrm{Num}(\partial A) \ (d = 2,\ \text{Non critical}) \tag{26}$$

where ∂A is the boundary of the subregion A, ϵ is UV lattice spacing, c is a positive constant which is proportional to the number of degrees of freedom of that field theory, and $\mathrm{Num}(\partial A)$ is the number of boundaries of A[24]. In particular, entanglement entropy is a divergent quantity in quantum field theory in general.

Entanglement entropy satisfies various important properties, inherited from von Neumann entropy,

$$S_A \geq 0 \text{ (Positivity)} \tag{27}$$

$$S_{A+B} + S_{B+C} \geq S_B + S_{A+B+C} \text{ (Strong subadditivity)} \tag{28}$$

$$S_A + S_B \geq S_{A+B} \text{ (Subadditivity)} \tag{29}$$

where $H = H_A \otimes H_B \otimes H_C$, and entanglement entropy is zero if and only if the state is pure.

There are number of applications of entanglement entropy in physics, in particular it is used to classify phase of quantum matter[25][26]. This is because entanglement entropy is a global quantity of a state, which can capture topological nature of ground state. In these applications, one can consider sum of entanglement entropy of subregions so that those divergent, non universal contributions cancel with each other.

Entanglement entropy is monotonically non increasing against Local Operations and Classical Communications (LOCC). Local operation is a transformation which acts locally on H_A and H_B. And classical communication is an exchange of classical bits between two systems, which is generically much cheaper than transfer of quantum bit since classical information can be amplified to any extent. More quantitatively, by classical communication, one can send the results of measurements at one system to another, and one can operate local operation which can depend on these results.

In general, it is known that any LOCC operation Λ can be written as following form;

$$\sum_i A^{i\dagger} \otimes B^{i\dagger} \cdot A^i \otimes B^i = I$$

$$\rho \to \Lambda(\rho) = \sum_i A^i \otimes B^i \rho A^{i\dagger} \otimes B^{i\dagger} \tag{30}$$

though not vice versa. The operators $A^i \otimes B^i$ are called Kraus operators. Operators satisfying this condition are called separable operations.

2.2.3 Axioms of bipartite entanglement measures

It is worth noting that entanglement entropy can not capture pure quantum entanglement. In other words, entanglement entropy also contains classical correlation, which is apparent when we consider thermal density matrix.

In this section, I will consider bipartite entanglement measures that can capture pure bipartite quantum entanglement. For this purpose, it is important to characterize and define quantitatively what are unentangled mixed states. It is clear that product states are unentangled states, so it is natural to define the states that can be obtained by LOCC from product states, as unentangled states. These states are called separable states. Bipartite entanglement measures capture how the state under consideration differs from separable states.

Equivalently, a quantum state ρ on $H = H_A \otimes H_B$ is called separable, if one can decompose ρ as

$$\rho = \sum_i p_i \sigma_A^i \otimes \tau_B^i \tag{31}$$

where

$$\sum_i p_i = 1 \tag{32}$$

with $p_i \geq 0$. And σ_A^i and τ_B^i are quantum states on H_A and H_B respectively[27].

One interesting necessary condition of separability is Positive Partial Transpose(PPT)[28]. For quantum state $\rho_{A,B}$ living on Hilbert space $H = H_A \otimes H_B$, we define partial transpose of $\rho_{A,B}^T$ by

$$\langle e^{(1)i}| \otimes \langle e^{(2)a}|\ \rho_{A,B}^T |e^{(1)j}\rangle \otimes |e^{(2)b}\rangle := \langle e^{(1)i}| \otimes \langle e^{(2)b}|\ \rho_{A,B} |e^{(1)j}\rangle \otimes |e^{(2)a}\rangle \tag{33}$$

where $|e^{(\alpha)i}\rangle$ denotes complete orthonormal basis of Hilbert space H_α. Note that the definition of partial transpose is independent from the choice of basis, as long as transformation matrix on basis is real.

The spectrum of partial transposed density matrix $\rho_{A,B}^T$ is independent from the choice of local basis and exchange between A and B. PPT condition requires the spectrum to be non negative. This condition is necessary condition for the separability of ρ_{AB}, and is indeed a necessary and sufficient condition in Hilbert spaces of the forms like $2 \otimes 2$ and $3 \otimes 3$.

Bipartite entanglement measure $E(\rho)$ is axiomatically defined to satisfy following properties (I)(II).

(I) Monotonicity of entanglement measure, is defined by the condition

$$E(\rho) \geq E(\Lambda(\rho)) \tag{34}$$

for any LOCC Λ. Note that for any finite dimensional bipartite system, we have the state that any state on that system can be obtained by LOCC on that state, called maximally entangled state. The monotonicity of bipartite entanglement implies that $E(\rho)$ is maximized on that state.

It is easy to see that local unitary transformation does not change $E(\rho)$.

(I') This condition is often satisfied by actual entanglement measures though it is not required, in order to be an entanglement measure. The statement is, for any LOCC such that

$$\Lambda(\rho) = \sum_i p_i \sigma_i \tag{35}$$

where $p_i \geq 0$ and σ_i are states, we have

$$E(\rho) \geq \sum_i p_i E(\sigma_i). \tag{36}$$

Clearly this condition is stronger than (I), since one can simply take $p_1 = 1$ and $\sigma_1 = \Lambda(\rho)$.

(II) For every separable state ρ,

$$E(\rho) = 0. \tag{37}$$

Note that by mapping from separable state to other separable state, one can show $E(\rho)$ must be constant on separable states only using property (I).

2.2.4 Various bipartite entanglement measures

One way to evaluate quantum entanglement of mixed state, is to calculate minimal distance between a set of separable states $\mathcal{S}$ which is closed under LOCC operations, and the given state. This can be realized by

$$E[\rho] := \inf_{\sigma \in \mathcal{S}} \mathcal{D}(\rho, \sigma). \tag{38}$$

for some distance function $\mathcal{D}$ satisfying

$$\mathcal{D}(\rho, \sigma) \geq \mathcal{D}(\Lambda(\rho), \Lambda(\sigma)), \tag{39}$$

for any LOCC Λ. It is easy to see that $E(\rho)$ indeed satisfies conditions of bipartite entanglement measure (I)(II). Also, if $\mathcal{D}$ satisfies

$$\mathcal{D}(\rho, \sigma) \geq \sum_{ii} p_i q_j \mathcal{D}(\Lambda(\rho_i), \Lambda(\sigma_j)). \tag{40}$$

for $\Lambda(\rho) = \sum_i p_i \rho_i$ and $\Lambda(\sigma) = \sum_j q_j \sigma_j$, it is clear that $E(\rho)$ satisfies the condition (I') as well. This stronger condition is known to be satisfied by square of Bures distance and relative entropy.

Relative entropy between ρ and σ is defined by

$$S(\rho || \sigma) = \mathrm{Tr}[\rho \log \rho] - \mathrm{Tr}[\rho \log \sigma]. \tag{41}$$

Relative entropy satisfies various important properties.

$$S(U\rho U^\dagger || U\sigma U^\dagger) = S(\rho||\sigma) \quad \text{(Unitary transformation)} \tag{42}$$

$$S(\rho_1 \otimes \rho_2 || \sigma_1 \otimes \sigma_2) = S(\rho_1||\sigma_1) + S(\rho_2||\sigma_2) \quad \text{(Additivity)} \tag{43}$$

$$S(\rho||\sigma) \geq 0 \quad \text{(Positivity)} \tag{44}$$

$$S(\rho||\sigma) \geq S(\Lambda(\rho)||\Lambda(\sigma)) \quad \text{(Monotonicity)} \tag{45}$$

where Λ is any completely positive trace-preserving map. Completely positive means, for any nonnegative integer k and k dimensional complex Hilbert space,

$$id_k \otimes \Lambda \tag{46}$$

maps positive operator to positive operator.

Bures distance is defined by

$$d_B(\rho, \sigma) = \Big(2(1 - \mathrm{Tr}[\sqrt{\rho^{1/2}\sigma\rho^{1/2}}])\Big)^{1/2}. \tag{47}$$

Bures distance indeed defines a distance on the manifold of quantum states. Bures distance satisfies several remarkable properties, it is monotonous under the action of completely positive trace preserving map Λ,

$$d_B(\Lambda(\rho), \Lambda(\sigma)) \leq d_B(\rho, \sigma). \tag{48}$$

Bures distance also bounds the trace distance from below and from above,

$$d_B(\rho, \sigma)^2 \leq \mathrm{Tr}[|\rho - \sigma|] \leq [1 - (1 - \frac{1}{2} d_B(\rho, \sigma)^2)^2]^{1/2}. \tag{49}$$

Further, Bures distance is joint convex, for $\eta_1 + \eta_2 = 1$ with $\eta_1,\ \eta_2 \geq 0$,

$$d_B(\eta_1\rho_1 + \eta_2\rho_2, \eta_1\sigma_1 + \eta_2\sigma_2) \geq \eta_1 d_B(\rho_1, \sigma_1) + \eta_2 d_B(\rho_2, \sigma_2). \tag{50}$$

Entanglement of formation

In general, if E is defined on pure states, one can generalize E to mixed states, by

$$E(\rho) = \inf_{\substack{\rho = \sum_i p_i |\psi_i\rangle\langle\psi_i| \\ \sum_i p_i = 1,\ p_i \geq 0}} \sum p_i E(|\psi_i\rangle). \tag{51}$$

This method of generating entanglement measure on mixed states is called convex roof. Note that we do not require $|\psi_i\rangle$ are orthogonal to each other. When one takes E as von Neumann entropy of reduced density matrix of pure states, $E(\rho)$ is called Entanglement of formation, and it is denoted as

$$E_F(\rho), \tag{52}$$

and it is known to satisfy conditions (I') and (II).

Distillable entanglement

Let us consider a Hilbert space $H^{(2)}$ spanned by two vectors $|0\rangle$ and $|1\rangle$ and its tensor product $H^{(2)} \otimes H^{(2)}$. The maximally entangled state

$$|\phi_2^+\rangle := \frac{|0\rangle|0\rangle + |1\rangle|1\rangle}{\sqrt{2}} \tag{53}$$

forms a Bell pair. One naive way to quantify bipartite entanglement is to count the number of Bell pairs between two systems, by acting LOCC on the system so that Bell pairs are manifest. Entanglement of distillation is designed to count such number of Bell pairs, but in copies of state under consideration.

Entanglement of distillation is defined by

$$E_D(\rho) = \lim_{n\to\infty} sup\Big(r : \inf_{\Lambda:LOCC} ||\Lambda(\rho^{\otimes n}) - (|\phi_2^+\rangle\langle\phi_2^+|)^{\otimes rn}||_1 = 0\Big) \tag{54}$$

which counts the number of Bell pairs in each ρ. Here we defined trace norm as $||A||_1 := \mathrm{Tr}|A| := \mathrm{Tr}\sqrt{A^\dagger A}$. One can show that entanglement of distillation satisfies (I') and (II).

Quantum mutual information

Quantum mutual information between systems A and B is defined by

$$I(A,B) := S(\rho_A) + S(\rho_B) - S(\rho_{AB}), \tag{55}$$

where ρ_{AB} is a quantum state on $H_A \otimes H_B$, and $\mathrm{Tr}_{H_A}\rho_{AB} = \rho_B$, $\mathrm{Tr}_{H_B}\rho_{AB} = \rho_A$. In terms of relative entropy, we can write

$$I(A,B) = S(\rho_{AB}||\rho_A \otimes \rho_B). \tag{56}$$

This implies many inequalities of relative entropy carries over to quantum mutual information. In particular, it is monotonically non increasing against completely positive trace preserving map. However, quantum mutual information is not zero unless $\rho_{AB} = \rho_A \otimes \rho_B$, which implies it is not zero even if ρ_{AB} is separable.

Negativity

Since partial transpose maps separable state into operator with nonnegative spectrum, one can quantify bipartite quantum entanglement by measuring negative spectrum of partial transposed density matrix.

Negativity is defined by the spectrum (λ_i) of partial transpose $\rho_{A,B}^T$ as

$$\mathcal{N}(\rho) = \sum_{i:\lambda_i<0} \lambda_i. \tag{57}$$

Note that $\mathrm{Tr}\rho_{A,B}^T = 1$. Logarithmic negativity is defined by

$$\mathcal{E}_{A,B}(\rho_{AB}) := \log\mathrm{Tr}|\rho_{A,B}^T| = \log(-2\mathcal{N}(\rho_{AB}) + 1), \tag{58}$$

and is designed to be additive. Note that negativity does not depend on choice of local basis nor exchange between A and B.

Note that negativity is zero if $\rho_{A,B}$ is separable, and also negativity and logarithmic negativity are monotonically non increasing under LOCC . It is known that logarithmic negativity gives an upper bound of distillable entanglement,

$$E_D(\rho_{AB}) \leq \mathcal{E}_{A,B}(\rho_{AB}). \tag{59}$$

Negativity can be computed using replica method[32]. Consider even integer n, then we have

$$\mathrm{tr}[(\rho_{AB}^T)^n|_{even\ n}] = \sum_\lambda \lambda^n = \sum_{\lambda>0} |\lambda|^n + \sum_{\lambda<0} |\lambda|^n, \tag{60}$$

therefore, if we analytically continue even integer n, we have

$$\mathcal{E}_{A,B}(\rho_{AB}) = \lim_{n\to 1} \mathrm{tr}[(\rho_{AB}^T)^n|_{even\ n}]. \tag{61}$$

In 2d conformal field theory, if we take subregions $A = [a_1,\ a_2]$ and $B = [b_1,\ b_2]$ at $t = 0$ with $a_2 \leq b_1$, we can express

$$\mathrm{tr}[(\rho_{AB}^T)^n|_{even\ n}] = \langle\sigma_n(a_1)\tilde{\sigma}_n(a_2)\tilde{\sigma}_n(b_1)\sigma_n(b_2)\rangle \tag{62}$$

using twist and anti twist operator. The conformal dimension of σ_n and $\tilde{\sigma}_n$ is

$$\Delta\sigma_n = \Delta\tilde{\sigma}_n = \frac{c}{12}(n - \frac{1}{n}), \tag{63}$$

and when two (anti)twist operators merge into one operator σ_n^2, the conformal dimension is, because the field moves from jth sheet to $j+2$th sheet when orbiting around the operator, and the Riemann surface decouples into two,

$$\Delta\sigma_n^2 = \Delta\tilde{\sigma}_n^2 = \frac{c}{6}(\frac{n}{2} - \frac{2}{n}). \tag{64}$$

This fact enables us to compute negativity for adjacent intervals. Since we have

$$\mathrm{tr}[(\rho_{AB}^T)^n|_{even\ n}] = \langle\sigma_n(-l_1)\tilde{\sigma}_n^2(0)\sigma_n(l_2)\rangle = c_n^2\frac{C_{\sigma_n\tilde{\sigma}_n^2\sigma_n}}{(l_1l_2)^{\Delta\sigma_n}(l_1+l_2)^{2\Delta\sigma_n-\Delta\tilde{\sigma}_n^2}}. \tag{65}$$

By taking the limit $n \to 1$, we obtain

$$\mathcal{E}_{AB} = \frac{c}{4}\log\frac{l_1l_2}{l_1+l_2} + \text{Const.} \tag{66}$$

Squashed entanglement

Another measure is (bipartite) Squashed entanglement $E_{sq}[\rho_{A,B}]$. It is defined by

$$E_{sq}[\rho_{A,B}] := \frac{1}{2}\inf_{\mathrm{Tr}_{H_E}\rho_{ABE}=\rho_{AB}} I(A:\ B|\ E) \tag{67}$$

where

$$I(A:B|\ E) := S(AE) + S(BE) - S(ABE) - S(E) \tag{68}$$

is the conditional mutual information for the extension $\rho_{A,B,E}$ which satisfies $\mathrm{Tr}_{H_E}\rho_{ABE} = \rho_{AB}$.

Squashed entanglement satisfies (I') and (II), as well as it is convex, so for any state ρ and σ and $0 < \lambda < 1$, we have

$$E_{sq}(\lambda\rho + (1-\lambda)\sigma) \leq \lambda E_{sq}(\rho) + (1-\lambda)E_{sq}(\sigma). \tag{69}$$

Note that if $I(A:B|\ E) = 0$ and dimension of total Hilbert space is finite, then ρ_{AB} is separable. Squashed entanglement is also super additive, namely

$$E_{sq}(\rho_{AA',BB'}) \geq E_{sq}(\rho_{A,B}) + E_{sq}(\rho_{A',B'}), \tag{70}$$

as well as additive on tensor product,

$$E_{sq}(\rho_{AA'} \otimes \rho_{BB'}) = E_{sq}(\rho_{A,B}) + E_{sq}(\rho_{A',B'}). \tag{71}$$

Squashed entanglement is bounded from above by entanglement of formation, and is bounded from below by distillable entanglement,

$$\frac{1}{2}(I(A:B) - S(AB)) \leq E_D(\rho_{AB}) \leq E_{sq}(\rho_{AB}) \leq E_F(\rho_{AB}). \tag{72}$$

Entanglement of purification

Entanglement of purification is defined by

$$E_P[\rho_{AB}] := \underset{\mathrm{Tr}_{H_{A'}\otimes H_{B'}}|\Psi\rangle\langle\Psi|=\rho_{AB}}{\mathrm{Min}} S_{|\Psi\rangle}(AA'). \tag{73}$$

Entanglement of purification is monotonously non increasing in the sense that for any completely positive trace preserving map Λ_A on H_A, we have

$$E_P((\Lambda_A \otimes I_B)(\rho_{AB})) \leq E_P(\rho_{AB}). \tag{74}$$

It is known that entanglement of purification is not necessarily zero even if ρ_{AB} is separable. There are several inequalities satisfied by entanglement of purification.

$$\begin{gathered}\frac{1}{2}I(A:B) \leq E_P(\rho_{AB}) \leq \min[S(\rho_A),\ S(\rho_B)] \\ E_P(\rho_{AB}) \leq E_P(\rho_{A(BC)}) \\ E_P(\rho_{A(BC)}) \geq \frac{1}{2}(I(A,B) + I(A,C)).\end{gathered} \tag{75}$$

3 Holographic dual of Fidelity susceptibility

One of the conceptual problems of holographic entanglement entropy is that, there exist regions in spacetime which Ryu-Takayanagi surface can not probe, even if we take arbitrary subregions. Such region in AdS is called entanglement shadow. Existence of entanglement shadow implies that, it is impossible to reconstruct AdS spacetime only from entanglement entropy of subregions at the boundary CFT. Therefore, it is necessary to seek for other information theoretic quantities which has gravity description. One interesting gravitational object is codimension one time slice in AdS. Such time slices inevitably probe the whole AdS spacetime, so there should be no issues such as entanglement shadow.

In this section, I will assert that, qualitative behavior of fidelity susceptibility can be captured by the volume of maximal volume codimension one time slice, based on [29]. I will compute fidelity susceptibility for static state via field theory as well as via holography. Then I will explain the proposal for holographic fidelity susceptibility, and compare the results with field theory results.

3.1 Fidelity susceptibility in field theory

In this thesis, we will focus on the fidelity susceptibility for pure states, though it can be defined for mixed states as well. Let us consider one parameter family of quantum states $|\Psi(\lambda)\rangle$. We consider inner product between $|\Psi(\lambda)\rangle$ and perturbed state $\lambda \to \lambda + \delta\lambda$. Then the fidelity susceptibility $G_{\lambda\lambda}$ is defined as follows:

$$|\langle\Psi(\lambda)|\Psi(\lambda+\delta\lambda)\rangle| = 1 - G_{\lambda\lambda}\cdot(\delta\lambda)^2 + O((\delta\lambda)^3). \tag{76}$$

The fidelity susceptibility measures the distance between quantum states with two infinitesimally different parameters. Because $|1-|\langle\Psi(\lambda_1)|\Psi(\lambda_2)\rangle||$ can be regarded as distance between two states, $G_{\lambda\lambda}$ defines a metric on the manifold of quantum states. This quantity diverges at quantum critical points and thus we can use it as an order parameter of quantum phase transitions (see e.g. [38]).

Now we introduce the fidelity susceptibility for ground states in QFT on R^{d+1}. We denote Euclidean time and space coordinates by τ and x. We consider the inner product $\langle\Omega_1|\Omega_2\rangle$ between two states $|\Omega_1\rangle$ and $|\Omega_2\rangle$. $|\Omega_i\rangle$ $(i = 1, 2)$ are ground states for the two Hamiltonians H_i $(i = 1, 2)$. We define their Euclidean Lagrangians by $\mathcal{L}_i$ $(i = 1, 2)$ and their partition functions by Z_i $(i = 1, 2)$. The inner product is described by the Euclidean path-integral:

$$\begin{aligned}&\langle\Omega_2|\Omega_1\rangle \\ &= (Z_1Z_2)^{-1/2}\int D\phi\exp[-\int d^dx(\int_{-\infty}^{0}d\tau\mathcal{L}_1 + \int_0^\infty d\tau\mathcal{L}_2)].\end{aligned} \tag{77}$$

Let us assume the difference $\mathcal{L}_2 - \mathcal{L}_1$ is infinitesimal and can be written by the operator $O(\tau, x)$ as

$$\mathcal{L}_2 - \mathcal{L}_1 \equiv \delta\mathcal{L} = \delta\lambda(x)\cdot O(\tau, x). \tag{78}$$

Then we rewrite (77) by using the expectation value of the operators in the vacuum state $|\Omega_1\rangle$:

$$\langle\tilde{\Omega}_2(\epsilon)|\Omega_1\rangle = \frac{\langle\exp[-\int_\epsilon^\infty d\tau\int d^dx\delta\mathcal{L}]\rangle}{(\langle\exp[-(\int_{-\infty}^{-\epsilon} + \int_\epsilon^\infty)d\tau\int d^dx\delta\mathcal{L}]\rangle)^{1/2}}, \tag{79}$$

where $\delta\mathcal{L} \equiv \mathcal{L}_2 - \mathcal{L}_1$. Here we introduced the UV regularization ϵ by replacing the ground state $|\Omega_2\rangle$ by

$$|\tilde{\Omega}_2(\epsilon)\rangle \equiv \frac{e^{-\epsilon H_1}|\Omega_2\rangle}{(\langle\Omega_2| e^{-2\epsilon H_1}|\Omega_2\rangle)^{1/2}}. \tag{80}$$

By performing perturbative expansions of (79) in λ up to quadratic terms, we obtain

$$\begin{aligned}&1 - \langle\tilde{\Omega}_2(\epsilon)|\Omega_1\rangle \\ &= \frac{1}{2}\int_{\epsilon}^{\infty} d\tau \int_{-\infty}^{-\epsilon} d\tau' \int d^d x \int d^d x' \langle \delta\mathcal{L}(\tau, x)\delta\mathcal{L}(\tau', x')\rangle,\end{aligned}$$

where we assumed the time reversal symmetry relation $\langle\delta\mathcal{L}(-\tau, x)\delta\mathcal{L}(-\tau', x')\rangle = \langle\delta\mathcal{L}(\tau, x)\delta\mathcal{L}(\tau', x')\rangle$.

In this way, the fidelity susceptibility with respect to the constant λ perturbation (78) can be computed as

$$G_{\lambda\lambda} = \frac{1}{2}\int_{\epsilon}^{\infty} d\tau \int_{-\infty}^{-\epsilon} d\tau' \int d^d x \int d^d x' \langle O(\tau, x) O(\tau', x')\rangle. \tag{81}$$

Note that up to now, our argument can be applied to any local operator O in any QFT. From now on, for simplicity, we will focus on the case where O is a scalar primary operator with total conformal dimension Δ.

The normalized two point function of the primary field is universal and given by

$$\langle O(\tau, x) O(\tau', x')\rangle = \frac{1}{((\tau-\tau')^2 + (x-x')^2)^{\Delta}}. \tag{82}$$

By plugging (82) into (81), when $d + 2 - 2\Delta < 0$ we obtain

$$G_{\lambda\lambda} = N_d \cdot V_d \cdot \epsilon^{d+2-2\Delta}, \tag{83}$$

where $N_d = \frac{2^{d-2\Delta}\pi^{d/2}\Gamma(\Delta-d/2-1)}{(2\Delta-d-1)\Gamma(\Delta)}$ and V_d is the infinite volume of R^d. In particular, we have $d+2-2\Delta = -d$ for marginal deformation. On the other hand, when $d+2-2\Delta \geq 0$, we have IR divergence in the integral, and we need an IR cut off L for both τ and x integrals. This leads us to $G_{\lambda\lambda} \propto V_d \cdot L^{d+2-2\Delta}$ for $d+2-2\Delta > 0$(agreeing with [38]), and $G_{\lambda\lambda} \propto V_d \cdot \log(L/\epsilon)$ for $d + 2 - 2\Delta = 0$.

3.2 Fidelity susceptibility in holography

In this section, I will argue that $G_{\lambda\lambda}$ in $d + 1$ dimensional holographic CFT deformed by an exactly marginal perturbation λ, is estimated by

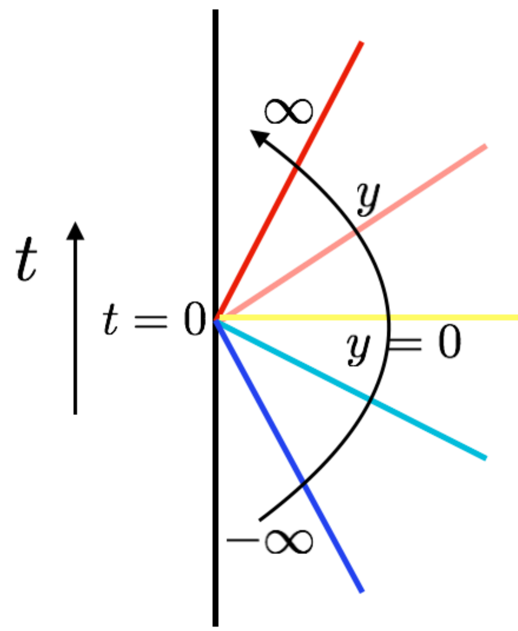

Figure 6: Janus geometry. Colored line corresponds to constant y slice of the geometry. The geometry interpolates two CFTs with different marginal couplings.

$$G_{\lambda\lambda} = n_d \cdot \frac{\mathrm{Vol}(\Sigma_{max})}{R^{d+1}}, \tag{84}$$

where n_d is an $O(1)$ positive constant and R is the radius of AdS. The surface Σ_{max} is the $d+1$ dimensional space-like time slice in the AdS, which ends on the time slice at the AdS boundary and has maximal volume among these timeslices.

Such maximal volume time slice can indeed probe entanglement shadow, therefore it conveys information of gravity different from Ryu-Takayanagi surface. There is another conjecture of CFT dual for such maximal volume as complexity of CFT state[34][35]).

In the case of CFT ground state with exactly marginal deformation, we can compute fidelity susceptibility from field theory and from AdS/CFT. In AdS/CFT computation, gravity backgrounds dual to both of $|\Omega_i\rangle$ $(i=1,2)$ are the pure AdS$_{d+2}$ with the same AdS radius R, since we are considering exactly marginal deformation. Such spacetime which interpolates two AdS spaces with different scalar couplings is called Janus solution [39]. The massless bulk scalar field which is dual to the exactly marginal operator O will be denoted by ϕ.

Let us study AdS$_3$ Janus solution introduced in [40]. The action is given by:

$$S = -\frac{1}{16\pi G_N}\int dx^3 \sqrt{g}\left(\mathcal{R} - g^{ab}\partial_a\phi\partial_b\phi + \frac{2}{R^2}\right). \tag{85}$$

The Janus solution is the metric

$$ds^2 = R^2 \left(dy^2 + f(y) ds^2_{AdS2}\right),$$
$$f(y) = \frac{1}{2}(1 + \sqrt{1-2\gamma^2}\cosh(2y)), \tag{86}$$

with the dilaton field

$$\phi(y) = \gamma \int_{-\infty}^{y} \frac{dy}{f(y)} + \phi_1, \tag{87}$$

where γ ($\leq \frac{1}{\sqrt{2}}$) is the parameter of the deformation, which is related to the difference between couplings of the two CFTs. The metric of AdS$_2$ slice is $ds^2_{AdS2} = (dz^2 + dx^2)/z^2$. $\phi_1 = \phi(-\infty)$ is dual to the coupling constant of the exactly marginal deformation for the ground state $|\Omega_1\rangle$, and the value $\phi_2 = \phi(\infty)$ for the other ground state $|\Omega_2\rangle$. ϕ_1 and ϕ_2 are related by

$$\phi_2 - \phi_1 = \sqrt{2}\arctan\left[\frac{1-\sqrt{1-2\gamma^2}}{\sqrt{2}\gamma}\right] \tag{88}$$

which is $\simeq \gamma$ when $\gamma \ll 1$. By comparing and matching the asymptotic behavior of the metric (86) at the infinity $y = y_\infty (\to \infty)$, which corresponds to the second CFT with marginal coupling ϕ_2, with the undeformed metric ($\gamma = 0$)

$$ds^2_{pure} = R^2 \left(d\hat{y}^2 + \frac{1}{2}(1 + \cosh(2\hat{y})) ds^2_{AdS2}\right), \tag{89}$$

one can find the following condition

$$\sqrt{1-2\gamma^2} e^{2y_\infty} = e^{2\hat{y}_\infty}. \tag{90}$$

On the other hand, the on-shell action of (85) is evaluated as

$$\begin{aligned} S(\gamma) \quad &= \frac{R}{4\pi G_N} V_{AdS_2} \cdot \int_{-y_\infty}^{y_\infty} dy \left\{\frac{1}{2}(1 + \sqrt{1-2\gamma^2}\cosh(2y))\right\} \\ &= \frac{R}{4\pi G_N} V_{AdS_2} \cdot \left\{ y_\infty + \frac{1}{2}\sqrt{1-2\gamma^2}\sinh(2y_\infty)\right\}, \end{aligned} \tag{91}$$

where $V_{AdS_2} = \int dx \int_\epsilon^\infty \frac{dz}{z^2} = \frac{V_1}{\epsilon}$ is the volume of AdS$_2$ with a unit AdS radius. Then by using the condition (90) at $y = y_\infty (\to \infty)$, we have

$$\begin{aligned} S(\gamma) - S(0) &= \frac{R}{4\pi G_N} V_{AdS_2} \cdot (y_\infty - \hat{y}_\infty) \\ &= \frac{RV_1}{16\pi G_N \epsilon} \cdot \log\left(\frac{1}{1-2\gamma^2}\right) > 0. \end{aligned} \tag{92}$$

For small γ^2, we finally find using GKPW relation

$$|\langle \Omega_2 | \Omega_1 \rangle| = e^{-(S(\gamma)-S(0))} \simeq 1 - \frac{RV_1}{8\pi G_N \epsilon}\gamma^2. \tag{93}$$

Therefore the fidelity susceptibility is estimated as

$$G_{\gamma\gamma} = \frac{cV_1}{12\pi\epsilon}, \tag{94}$$

where we used the holographic relation for $d = 2$ CFT central charge

$$c = \frac{3R}{2G_N}. \tag{95}$$

Since the normalization convention of scalar field in (85) leads the two point function of O to be proportional to c (i.e. $\delta\lambda \propto \sqrt{c}\delta\phi = \sqrt{c}\gamma$) , we indeed obtain the formula (84), where Σ is the AdS_2 slice $\rho = 0$ in pure AdS_3.

To generalize and to study higher dimensional, time dependent fidelity susceptibility universally, I will consider a simple holographic model, which turns out to give an excellent (hard wall) approximation to various examples including time dependent cases. Although fidelity susceptibility for ground states is simply given by integration of two point function, it is not an easy task to generalize the arguments to general time dependent cases. However, with the holographic model I will propose from now on, can be computed in straight forward manner and indeed gives consistent result with known field theory calculations.

Let me first approximate sudden change of exactly marginal deformation in CFT_{d+1}, which can be considered as defect in CFT, by a $d+1$ dimensional defect brane Σ with a tension T at $\tau = 0$ timeslice. Holographically, such defect brane extends to the bulk, from the AdS boundary. This is similar to the holographic constructions in [41, 42, 43], to the hard wall model of AdS/QCD [44]. Therefore it should be regarded as a phenomenological model rather than a precise prediction from AdS/CFT with controllable approximation.

In the gravity setup such prescription is realized by adding the defect brane action

$$S_{brane} = T\int_\Sigma \sqrt{g}, \tag{96}$$

to the Einstein-Hilbert action. This prescription is consistent with the boundary (or defect) conformal symmetry in a similar way to that of AdS/BCFT [43].

Again we can describe the perturbation (78) by the profile of a massless scalar field ϕ. When the deformation $\delta\lambda$ is infinitesimally small, we have

$$T \simeq n_d \cdot \frac{(\delta\lambda)^2}{R_{AdS}^{d+1}}, \tag{97}$$

where n_d is an $O(1)$ constant which is fixed from the normalization of two point function (82). The Einstein equation shows that T is proportional to $(\delta\lambda)^2$, as the bulk stress tensor is quadratic with respect to the scalar field. The dependence on R can be explained by the dimensional reason or by comparing with the Janus computation. In this limit, we can treat the brane as a probe, ignoring its back-reaction. Finally we impose the equation of motion with respect to the brane embedding. This requires that the action (96) is extremal and thus in the Lorentzian signature, Σ is the maximal area surface Σ_{max} which ends on the time slice $\tau = 0$ at the AdS boundary. Together with (97), we reach our claim (84).

For CFT$_{d+1}$ on R^{d+1}, the holographic prescription (84) leads us to

$$G_{\lambda\lambda} \;=\; n_d V_d \int_\epsilon^\infty \frac{dz}{z^{d+1}} = \frac{n_d V_d}{d\epsilon^d}, \tag{98}$$

which indeed agrees with the CFT result (83).

Similarly we can analyze the global AdS$_{d+2}$ also. Global AdS is described by the metric

$$ds^2 = R^2\left(-(r^2+1)dt^2 + \frac{dr^2}{r^2+1} + r^2 d\Omega_d^2\right). \tag{99}$$

Then the fidelity susceptibility for a CFT$_{d+1}$ on $R \times S^d$ is

$$G_{\lambda\lambda} = n_d V_d \int_0^{r_\infty} \frac{r^d}{\sqrt{r^2+1}} dr = \frac{n_d V_d}{d\epsilon^d} + \cdots, \tag{100}$$

where $r_\infty \sim 1/\epsilon$ corresponds to the UV cut off of the CFT. It is clear from (100) that $G_{\lambda\lambda}$ is smaller than that of flat space (98), due to the mass gap in CFTs on a compact space.

Another interesting example is the AdS Schwarzschild black hole, whose metric is given by

$$ds^2 = R^2\left(\frac{dz^2}{h(z)z^2} - \frac{h(z)}{z^2}dt^2 + \frac{\sum_{i=1}^d dx_i^2}{z^2}\right), \tag{101}$$

$$h(z) \equiv 1 - (z/z_0)^{d+1}, \tag{102}$$

and which is dual to the finite temperature CFT. The parameter z_0 is related the temperature T by $z_0 = \frac{d+1}{4\pi T}$. The fidelity susceptibility is computed as

$$G_{\lambda\lambda} = n_d V_d \int_\epsilon^{z_0} \frac{dz}{\sqrt{h(z)} z^{d+1}} \tag{103}$$

$$= \frac{n_d V_d}{d} \left(\frac{1}{\epsilon^d} + \frac{b_d}{z_0^d} \right), \tag{104}$$

$$b_d \equiv -1 + d \int_0^1 dy \left(1 - y^{d+1} + \sqrt{1 - y^{d+1}} \right)^{-1} \tag{105}$$

$$= (d-1) \frac{\sqrt{\pi}}{2} \frac{\Gamma\left(1 + \frac{1}{d+1}\right)}{\Gamma\left(\frac{1}{2} + \frac{1}{d+1}\right)} \geq 0. \tag{106}$$

For example, we have $b_1 = 0$, $b_2 \simeq 0.70$, $b_3 \simeq 1.31$.

In this thermal example (106), we are actually considering fidelity susceptibility for mixed states. The fidelity susceptibility for mixed state can be defined in several ways. One possibility is

$$\frac{\mathrm{Tr}[\rho(\lambda)\rho(\lambda + d\lambda)]}{\sqrt{\mathrm{Tr}[\rho(\lambda)^2]\mathrm{Tr}[\rho(\lambda + d\lambda)^2]}} = 1 - 2G_{\lambda\lambda}(\delta\lambda)^2. \tag{107}$$

Also it can be defined by relative entropy

$$S(\rho(\lambda)||\rho(\lambda + d\lambda)) = G_{\lambda\lambda}(\delta\lambda)^2. \tag{108}$$

In general those definitions of distance between states are not equivalent to each other, so we have ambiguity in generalizing our holographic formula for mixed states, though these definitions are equivalent for pure states. However, we can describe the thermal state as a pure state in the doubled Hilbert space by purification. In this equivalent description, our result (106) can be interpreted as (a half of) the fidelity susceptibility for the purified state as we will see later.

Finally we study a time-dependent example in order to confirm our holographic prescription (84) can be applied to such non-trivial setup. For this objective, we consider thermo-field double (TFD) state in a two dimensional (2d) CFT:

$$|\Psi_{TFD}(t)\rangle \propto e^{-i(H^{(A)}+H^{(B)})t} \sum_n e^{-\frac{\beta}{4}(H^{(A)}+H^{(B)})} |n\rangle_A |n\rangle_B, \tag{109}$$

where $H^{(A)}$ and $H^{(B)}$ are the identical Hamiltonians for the first and the second CFT, and

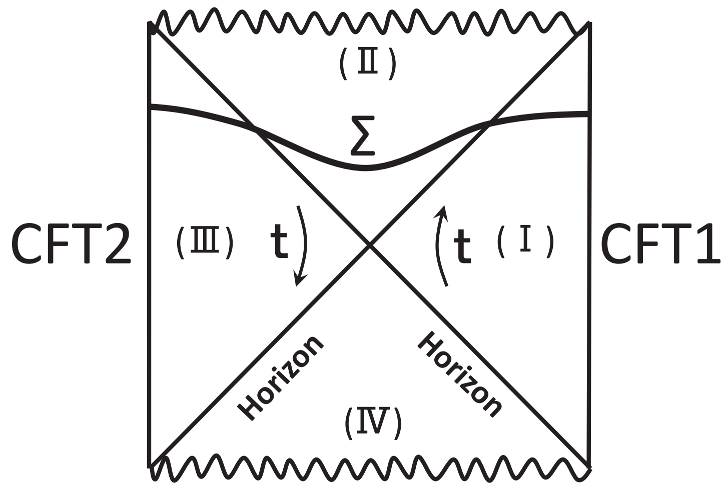

Figure 7: A time slice in the Penrose diagram of eternal AdS black hole which connects the two boundaries dual to the thermofield doubled CFTs.

the states $|n\rangle_{A,B}$ are the normalized energy eigenstates in each CFTs. Tracing out one CFT Hilbert space yields thermal mixed state with inverse temperature β in another CFT. This TFD system is dual to the maximally extended eternal AdS black hole depicted in Fig.7.

We are interested in the overlap

$$\langle \Psi'_{TFD}(t)|\Psi_{TFD}(t)\rangle \tag{110}$$

and the fidelity susceptibility

$$G_{\lambda\lambda}. \tag{111}$$

Here, the state $\langle \Psi'_{TFD}(t)|$ is the TFD state, and it evolves with the Hamiltonian $H'^{(A)}+H'^{(B)}$ deformed by infinitesimal exactly marginal λ-perturbation (78) on each of $H^{(A)}$ and $H^{(B)}$ simultaneously. We argue that this deformation is dual to introducing a defect brane Σ in the two sided black hole as in Fig.7. Note that the defect brane connects two boundaries, through the Einstein-Rosen bridge.

Let us compute $G_{\lambda\lambda}$ purely from Euclidean path-integral in 2d CFT. Two point function on $S^1 \times R$, where S^1 is the thermal circle whose periodicity is β, is

$$\langle O(x_1,\tau_1)O(x_2,\tau_2)\rangle = \frac{\left(\frac{\pi}{\beta}\right)^{2\Delta}}{\left(\sinh^2\left(\frac{\pi(x_1-x_2)}{\beta}\right)+\sin^2\left(\frac{\pi(\tau_1-\tau_2)}{\beta}\right)\right)^{\Delta}}.$$

Then, $G_{\lambda\lambda}$ at the Euclidean time τ is expressed as

$$G_{\lambda\lambda}=\frac{1}{2}\int_{-\infty}^{\infty}dx_1dx_2\int_{\frac{\beta}{4}+\tau+\epsilon}^{\frac{3\beta}{4}-\tau-\epsilon}d\tau_2\int_{-\frac{\beta}{4}-\tau+\epsilon}^{\frac{\beta}{4}+\tau-\epsilon}d\tau_1\langle O(x_1,\tau_1)O(x_2,\tau_2)\rangle. \tag{112}$$

Using the formula (for $0\leq t\leq \pi$)

$$\int_{-\infty}^{\infty}dx\left(\sinh^2 x+\sin^2 t\right)^{-2}=\frac{1}{\sin^2 t\cdot\cos^2 t}+(t-\pi/2)\cdot\frac{2\sin^2 t-1}{\sin^3 t\cos^3 t}, \tag{113}$$

we can evaluate the fidelity susceptibility (112) when $\Delta=2$, up to finite terms in the $\epsilon\to 0$ limit. It is given by

$$G_{\lambda\lambda}=\frac{\pi V_1}{8\epsilon}-\frac{\pi V_1}{2\beta}+\frac{2\pi^2 V_1}{\beta^2}\cdot\tau\cot\left(\frac{4\pi\tau}{\beta}\right). \tag{114}$$

When $\tau=0$, we simply find $G_{\lambda\lambda}=\frac{\pi V_1}{8\epsilon}$. This is consistent with the holographic result $b_1=0$ in (106).

To study fidelity susceptibility in real time, we need to analytically continue the Euclidean time $\tau\to it$, and we obtain

$$G_{\lambda\lambda}=\frac{\pi V_1}{8\epsilon}-\frac{\pi V_1}{2\beta}+\frac{2\pi^2 V_1}{\beta^2}\cdot\frac{\cosh\frac{4\pi t}{\beta}}{\sinh\frac{4\pi t}{\beta}}\cdot t. \tag{115}$$

At late time $t\gg\beta$, it grows linearly

$$G_{\lambda\lambda}\simeq\frac{\pi V_1}{8\epsilon}+\frac{2\pi^2 V_1}{\beta^2}\cdot t. \tag{116}$$

We now turn to the holographic computation in the two sided black hole, where the region (I) in Fig.7 is described by the metric (we set $\beta=2\pi$ for simplicity)

$$ds^2=R^2(-\sinh^2\rho dt^2+d\rho^2+\cosh^2\rho dx^2). \tag{117}$$

We can continue into the region (II) by analytically continuation $\kappa=-i\rho$ and $\tilde{t}=t+\frac{\pi i}{2}$. In the region (II), if we parametrize Σ by $\kappa=\kappa(\tilde{t})$ of Σ, its volume is

$$\mathrm{Vol}(\Sigma) = R^2 V_1 \int d\tilde{t} \cos\kappa \sqrt{\sin^2\kappa - (\partial\kappa/\partial\tilde{t})^2}. \tag{118}$$

We define κ_* $(0 \le \kappa_* < \pi/4)$ as the value of κ when $\partial\kappa/\partial\tilde{t} = 0$. We can maximize the volume (118) and extend the solution into the region (I) in a similar way as in [46]. Finally, we obtain the following expression of $\mathrm{Vol}(\Sigma_{max})$ as a function of t, in terms of the parameter κ_*

$$\frac{\mathrm{Vol}(\Sigma)}{R^{d+1}V_1} = 2\sinh\rho_\infty + 2\int_0^{\kappa_*} d\kappa \frac{\cos\kappa}{\sqrt{\sin^2(2\kappa_*)/\sin^2(2\kappa) - 1}} \tag{119}$$

$$-2\int_0^{\rho_\infty} d\rho \frac{\cosh\rho\left(\sqrt{\sinh^2(2\rho)+\sin^2(2\kappa_*)} - \sinh(2\rho)\right)}{\sqrt{\sinh^2(2\rho)+\sin^2(2\kappa_*)}}, \tag{120}$$

$$t = \int_0^{\kappa_*} \frac{d\kappa}{\sin\kappa\sqrt{1-\sin^2(2\kappa)/\sin^2(2\kappa^*)}} \tag{121}$$

$$-\int_0^{\rho_\infty} \frac{d\rho}{\sinh\rho\sqrt{1+\sinh^2(2\rho)/\sin^2(2\kappa^*)}}, \tag{122}$$

where ρ_∞ is corresponding to the UV cut off, and is given by $e^{\rho_\infty} \propto 1/\epsilon$. In late time (i.e. $\kappa_* \to \pi/4$) we find the finite part

$$\frac{\mathrm{Vol}_{finite}(\Sigma)}{R^{d+1}} \underset{\kappa_*\to\pi/4}{\to} V_1 \cdot t, \tag{123}$$

which agrees with $2G_{\lambda\lambda}$ in (116). This linear t growth comes from the growth of Einstein-Rosen bridge as already noted in [34]. In Fig.8 we plotted the holographic result versus the CFT result. In the plot, we have order one deviation numerically, but the deviation is small. Moreover, the holographic result reproduces the CFT result qualitatively, and late time behavior coincide exactly as we noted earlier. The deviation exist in early time, in the limit $t \to 0$ (or $\kappa_* \to 0$) we find $\mathrm{Vol}_{finite}(\Sigma)/(R^{d+1}V_1) \simeq \frac{2}{\pi}t^2$, while $2G_{\lambda\lambda}/V_1 \simeq \frac{2}{3}t^2$, so there is an order one, but tiny deviation in early time.

Note that the holographic prescription (84) computes the fidelity susceptibility at each time. In the standard AdS/CFT, the original, undeformed gravitational spacetime and deformed one are dual to each corresponding quantum states: $|\Psi(\lambda,t)\rangle$ and $|\Psi(\lambda+\delta\lambda,t)\rangle$, which are time evolved by two infinitesimally different Hamiltonians. The fidelity susceptibility is defined by taking the inner product of these two states at each time.

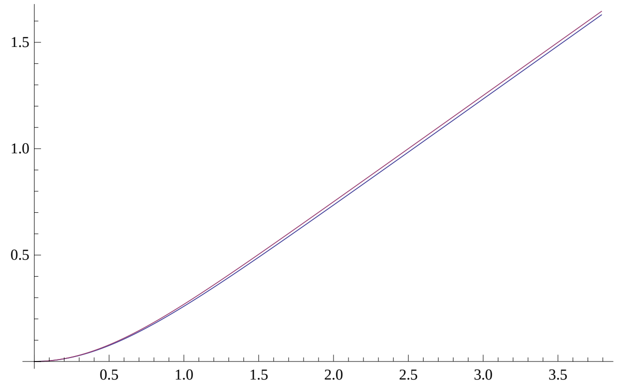

Figure 8: We compare the finite part of our holographic result $\mathrm{Vol}(\Sigma)/(R^{d+1}V_1)$ (blue) with that of our CFT result $2G_{\lambda\lambda}/V_1$ (red) as a function of the time t for the TFD state. They deviates only slightly. We set $\beta = 2\pi$.

In summary, in this section, I introduced fidelity susceptibility in CFTs and proposed its holographic formula based on a simple probe, hard wall model. I presented non-trivial evidence supporting the proposal.

4 Relation between fidelity susceptibility and quantum chaos

The study of chaos in terms of AdS/CFT correspondence [9] has revealed new perspectives on quantum field theory and gravity. Its relations to black hole information paradox [47] [48] and Fast scrambling conjecture [49][50][51] are particularly interesting.

Let us consider scrambling of local excitation. Let me consider a thermal system at equilibrium is excited by a local operator W. Sometime after the excitation, the excitation will lose its identity, so that it can not be distinguished from other excitations by local measurement. We can distinguish these states only by measuring total system, so in such case the excitation is called scrambled. One way to measure indistinguishability quantitatively is to measure complexity of the excitation $W(t)$. When the perturbation $W(-t_w)$ is scrambled, then it should be a complicated sum of a varieties of local operators, which is hard to distinguish from other scrambled operator as long as one is focussing on small number of coefficients. One way to measure complexity of operators is via growth of expectation value of commutator square

$$\langle [W(t),\ V][W(t),\ V]^{\dagger}\rangle_{\beta} \tag{124}$$

for all local V with $[W,\ V] = 0$. The expectation value is small at early time, and grows as $e^{\lambda_L t}$ at late time, where λ_L is called Lyapunov exponent. Such growth of commutators was first considered in [52], and was interpreted as diagnosis of chaos recently, because semiclassically, the commutator $\langle[q(t),\ p(0)][q(t),\ p(0)]^{\dagger}\rangle$ is equal to the square of Poisson bracket

$$\{q(t),\ p(0)\}_P^2 = (\frac{\delta q(t)}{\delta q(0)})^2, \tag{125}$$

whose exponential growth implies high sensitivity of trajectories to initial configurations. In this case, Lyapunov exponent from the commutator square is equal to twice the Lyapunov exponent in classical mechanics. λ_L is known to obey a bound $\lambda_L \leq \frac{2\pi}{\beta}$ in large N theory [51]. The bound is saturated by the holographic CFT dual to classical Einstein gravity [50][53][54][55][56][57]. The dual geometry in this case is approximated by shock wave geometry. Lyapunov exponents of various theories are computed in [58][59][60][61][62][63][64]. Related studies include [65][66][67][68][69][70][71][72].

In this section, I will characterize scrambling of operator by fidelity susceptibility based on [30]. As I will explain later, Loschmodt echo, which is closely related to fidelity susceptibility, is known to be a useful tool to study chaos in quantum systems [73][74][75][76][77][78][79][80][81][82], though the relation to what I describe here is yet unclear.

Let us discuss quantum chaos from the view point of "initial condition sensitivity". When two slightly different states evolve with the identical Hamiltonians, the inner product between two states is conserved because of the linearity and the unitarity of quantum mechanics, so there is no "butterfly effect". Nonetheless, butterfly effect can play role when we evolve two states with slightly different Hamiltonians $H_\lambda = H_0 + \lambda V$ and $H_{\lambda+\delta\lambda} = H_0 + (\lambda + \delta\lambda)V$. λ represents a coupling of external environment or internal imperfections. In this case, the inner product

$$|\langle\psi_{\lambda+\delta\lambda}|e^{iH_{\lambda+\delta\lambda}t}e^{-iH_\lambda t}|\psi_\lambda\rangle| \tag{126}$$

is not conserved in general, and it decays rapidly if H_λ is "chaotic" as in fig (9). The decay of fidelity signifies difficulty of revival of quantum state by imperfect time reversal procedure, and is also a measure of the strength of decoherence when we consider the deformation as external one.

In this section, we consider time evolution of distance between thermal states excited by local operator, with slightly different Hamiltonians. Assuming the difference between two Hamiltonians is infinitesimally small, we find that the distance for short time is proportional to expectation value of commutator square of local operators. This implies that, the rapid growth of distance signifies the scrambling. In particular, in large N chaotic theory, we show that growth of Fisher information metric is proportional to $e^{\frac{2\pi}{\beta}t}$, by using holographic prescription for fidelity susceptibility. Intuitive interpretation of our result is that, the trajectory of thermal states excited by local operator is highly sensitive to external environment or internal imperfections, and it is easy to deviate. This can be considered as diagnosis of butterfly effect. In addition, I note that the formula we study is equal to holographic two point Wilson loop. We confirmed that it decays rapidly, as expected from holographic quantum chaos.

4.1 Fidelity susceptibility in chaotic system

In this section, we point out that growth of fidelity susceptibility of thermofield double states, perturbed by local operators, corresponds to growth of commutator between excitation and external perturbation. This growth of commutators implies that the initial excitation is scrambled.

We consider time evolution of fidelity susceptibility of excited states. We consider the inner product of two excited states with different Hamiltonians,

$$|\Psi_\lambda(t)\rangle = e^{-iH_\lambda t} A e^{iH_\lambda t} |\psi_\lambda\rangle, \tag{127}$$

$$|\Psi_{\lambda+\delta\lambda}(t)\rangle = e^{-iH_{\lambda+\delta\lambda} t} A e^{iH_{\lambda+\delta\lambda} t} |\psi_{\lambda+\delta\lambda}\rangle, \tag{128}$$

so that

$$\langle \Psi_{\lambda+\delta\lambda}(t) | \Psi_\lambda(t)\rangle = \langle \psi_{\lambda+\delta\lambda} | e^{-iH_{\lambda+\delta\lambda} t} A e^{iH_{\lambda+\delta\lambda} t} e^{-iH_\lambda t} A e^{iH_\lambda t} |\psi_\lambda\rangle. \tag{129}$$

The decay of this inner product can be understood as diagnosis of butterfly effect. When $|\psi\rangle = |\psi_\lambda\rangle = |\psi_{\lambda+\delta\lambda}\rangle$, and $|\psi\rangle$ is an eigenstate of A, there is a related quantity called Polarization echo, which is given by

$$\langle \psi_\lambda | e^{iH_{\lambda+\delta\lambda} t} e^{-iH_\lambda t} A e^{iH_\lambda t} e^{-iH_{\lambda+\delta\lambda} t} A |\psi_\lambda\rangle. \tag{130}$$

Polarization echo can be used to measure the distance between a state $e^{iH_\lambda t} e^{-iH_{\lambda+\delta\lambda} t}|\psi_\lambda\rangle$ and eigenspace of A which $|\psi_\lambda\rangle$ belongs to.

Polarization echo and related quantities are studied and measured in various experiments, including Nuclear Magnetic Resonance, Microwave billiards, Elastic waves in metals, and so on.

Fidelity susceptibility is a useful tool in quantum estimation theory, in particular, its reciprocal gives lower bound of variance of an estimate of deterministic parameter in Cramer-Rao bound. Namely, if we have one parameter family of states $|\Psi_\lambda\rangle$, and $\hat{\lambda}$ is Hermitian operator which satisfies $\lambda = \langle \Psi_\lambda | \hat{\lambda} | \Psi_\lambda \rangle$, then we have

$$\langle \Psi_\lambda | (\hat{\lambda} - \lambda)^2 | \Psi_\lambda \rangle \geq \frac{1}{8 G_{\lambda\lambda}}. \tag{131}$$

Also, it is known that it can be used as diagnosis of non-Markovianity [83][84].

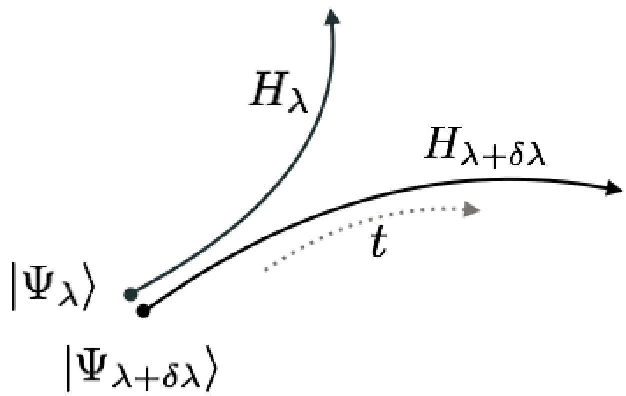

Figure 9: Orbits of states with slightly different Hamiltonians. For chaotic theory or chaotic perturbation to the original Hamiltonian, the distance between states grows exponentially even if original states are the same or close to each other.

Thermofield double (TFD) state of a QFT is defined as a purification of thermal density matrix. Explicitly, it is defined by

$$|\Psi_{\rm TFD}\rangle = \frac{1}{\sqrt{Z(\beta)}}\sum_i e^{-\frac{\beta E_i}{2}}|E_i\rangle_L \otimes |E_i\rangle_R, \tag{132}$$

where β is the inverse temperature and $|E_i\rangle$s are eigenstates of QFT Hamiltonian.

The TFD state lives in tensor product of two identical QFT Hilbert spaces with identical Hamiltonians, and tracing out either side of Hilbert space gives the thermal density matrix $\rho(\beta)$ of the system, with the inverse temperature β. Time evolution of the TFD state is given by

$$\begin{aligned} |\Psi_{\rm TFD}(t)\rangle \quad &= e^{-i(H_L+H_R)t}|\Psi_{\rm TFD}\rangle \\ &= \frac{1}{\sqrt{Z(\beta)}}\sum_i e^{-(\frac{\beta}{2}+2it)E_i}|E_i\rangle_L \otimes |E_i\rangle_R, \end{aligned} \tag{133}$$

where $Z(\beta)$ is thermal partition function. We consider scalar excitation W at $t = -t_w$ on TFD state, which lives in left QFT Hilbert space. Then the excited TFD state at $t = 0$ is given by

$$|\Psi_{\rm TFD}(\lambda, W)\rangle = \frac{1}{\sqrt{Z_W(\beta)}} e^{-iH^\lambda_{tot}t_w} W e^{iH^\lambda_{tot}t_w}|\Psi_{\rm TFD}(\lambda)\rangle, \tag{134}$$

with $H_{tot} = H_L + H_R$. Tracing out right Hilbert space of this state gives the excited thermal density matrix

$$e^{-iH^{\lambda}t_w}We^{iH^{\lambda}t_w}\rho(\beta)e^{-iH^{\lambda}t_w}We^{iH^{\lambda}t_w}. \tag{135}$$

It is known that Bures distance of mixed states ρ, σ is given by

$$d_B(\rho,\sigma)=\underset{|\Psi_\rho\rangle,\ |\Psi_\sigma\rangle}{\mathrm{Min}}\, d_B(|\Psi_\rho\rangle,\ |\Psi_\sigma\rangle) \tag{136}$$

where $|\Psi_\rho\rangle$, $|\Psi_\sigma\rangle$ are purification of ρ and σ living in the same extended Hilbert space. Therefore, fidelity susceptibility of excited TFD state gives upper bound on Bures metric of excited thermal density matrices.

Let's consider deformation parametrized by coupling λ, of the QFT Hamiltonian. Then the inner product and the fidelity susceptibility of TFD state $|\mathrm{TFD}(t,\lambda)\rangle$ corresponding to (129) with $|\psi\rangle\neq|\psi'\rangle$ is given by

$$|\langle\Psi_{\mathrm{TFD}}(\lambda+\delta\lambda,W)|\Psi_{\mathrm{TFD}}(\lambda,W)\rangle|=1-G_{\lambda\lambda}(\delta\lambda)^2+O((\delta\lambda)^3). \tag{137}$$

We assume that the theory has time reversal symmetry. Then

$$\begin{aligned}&|\langle\Psi_{\mathrm{TFD}}(\lambda+\delta\lambda,W)|\Psi_{\mathrm{TFD}}(\lambda,W)\rangle|\\&=\frac{1}{\sqrt{Z_W(\beta,\lambda)Z_W(\beta,\lambda+\delta\lambda)}}|\mathrm{Tr}\Big[e^{-\frac{\beta}{2}H_L^{\lambda+\delta\lambda}}W^{\lambda+\delta\lambda}(-t_w)W^{\lambda}(-t_w)e^{-\frac{\beta}{2}H_L^{\lambda}}\Big]|,\end{aligned} \tag{138}$$

where we defined $W^{\lambda}(t)=e^{iH^{\lambda}t}We^{-iH^{\lambda}t}$. The fidelity susceptibility can be decomposed into two parts,

$$G_{\lambda\lambda}=G^{(W:0)}_{\lambda\lambda}+G^{(W:c)}_{\lambda\lambda}, \tag{139}$$

where

$$\begin{aligned}G^{(W:0)}_{\lambda\lambda}=\quad&\frac{1}{2}\int_0^{\beta}\underset{t_1>\frac{\beta}{2}>t_2}{dt_1dt_2}\,\mathrm{Tr}\Big[\frac{e^{-\beta H}}{Z_W(\beta,\lambda)}e^{Ht_1}Ve^{-Ht_1}e^{Ht_2}Ve^{-Ht_2}W(-t_w)^2\Big]\\&-\frac{3}{8}\Big(\int_0^{\beta}dt\mathrm{Tr}\Big[\frac{e^{-\beta H}}{Z_W(\beta,\lambda)}e^{Ht}Ve^{-Ht}W(-t_w)^2\Big]\Big)^2,\end{aligned} \tag{140}$$

$$
\begin{aligned}
G^{(W:c)}_{\lambda\lambda} = \quad & \mathrm{Re}\Big[\frac{1}{2}\int_0^{t_w} dt_1 dt_2 \mathrm{Tr}\Big[\frac{e^{-\beta H}}{Z_W(\beta,\lambda)}\Big[W(-t_w),\ V(-t_1)\Big]\cdot\Big[W(-t_w),\ V(-t_2)\Big]^\dagger\Big] \\
& +\frac{i}{2}\int_0^{\frac{\beta}{2}} dt_E \int_0^{t_w} dt \mathrm{Tr}\Big[\frac{e^{-\beta H}}{Z_W(\beta,\lambda)} e^{Ht_E} V e^{-Ht_E}\Big[\ \Big[W(-t_w),\ V(-t)\Big],\ W(-t_w)\Big]\Big]\ \Big] \\
& -\frac{1}{2}\Big(\int_0^{t_w} dt \mathrm{Tr}\Big[\frac{e^{-\beta H}}{Z_W(\beta,\lambda)}\Big[W(-t_w),\ V(-t)\Big]\ W(-t_w)\Big]\Big)^2. \qquad (141)
\end{aligned}
$$

$G^{(W:c)}_{\lambda\lambda}$ is negligible when the theory is not chaotic, so that $[W(-t_w),\ V(-t)] \approx 0$ holds. Therefore, the exponential growth of $G^{(W:c)}_{\lambda\lambda}$ implies scrambling of the excitation W.

Let us consider the large N limit. The relaxation time t_r of a thermal QFT can be determined from the behavior of Lorentzian two point function

$$
\langle W(t)W(0)\rangle \sim \mathcal{O}(e^{-\frac{t}{t_r}}). \qquad (142)
$$

In holographic CFT, t_r is given by β, which is significantly small compared to the scrambling time $t_s = \frac{\beta}{2\pi}\log N^2$. We consider particular class of large N QFT with such hierarchy.

In [51], it was shown that CFT dual to Einstein gravity has largest Lyapunov exponent, among the large N theories with such hierarchy in scrambling time and relaxation time.

Under these assumptions, when $t_w >> t_r$, we have

$$
G^{(W:0)}_{\lambda\lambda} \underset{t_w>>t_r}{\approx} \frac{1}{2}\int_0^{\beta} \underset{t_1>\frac{\beta}{2}>t_2}{dt_1 dt_2}\ \mathrm{Tr}\big[\frac{e^{-\beta H}}{Z(\beta,\lambda)} e^{Ht_1} V e^{-Ht_1} e^{Ht_2} V e^{-Ht_2}\big]. \qquad (143)
$$

Therefore, $G^{(W:0)}_{\lambda\lambda}$ coincides with fidelity susceptibility of unexcited TFD state. In particular, $G^{(W:0)}_{\lambda\lambda}$ is independent from excitation W and is time independent. This fact implies that growth of fidelity susceptibility at late time $t_w >> t_r$ comes purely from scrambling in large N theory.

We can also consider similar quantity, corresponding to (129) with $|\psi\rangle = |\psi'\rangle$, which purely contains chaotic contributions in the former Fidelity susceptibility. We consider the inner product of two states

$$
|\Psi_{\mathrm{TFD}}(\lambda, W)\rangle = \frac{1}{\sqrt{Z_W(\beta)}} e^{-iH^{\lambda}_{tot}t_w} W e^{iH^{\lambda}_{tot}t_w} |\Psi_{\mathrm{TFD}}(\lambda)\rangle, \qquad (144)
$$

$$
|\Psi_{\mathrm{TFD}}(\lambda, \delta\lambda, W)\rangle = \frac{1}{\sqrt{Z_W(\beta,\delta\lambda)}} e^{-iH^{\lambda+\delta\lambda}_{tot}t_w} W e^{iH^{\lambda+\delta\lambda}_{tot}t_w} |\Psi_{\mathrm{TFD}}(\lambda)\rangle, \qquad (145)
$$

where $Z_W(\beta, \delta\lambda)$ is the normalization constant. Infinitesimal part of the inner product is defined by

$$\begin{aligned}
&|\langle \Psi_{\mathrm{TFD}}(\lambda, W)|\Psi_{\mathrm{TFD}}(\lambda, \delta\lambda, W)\rangle| \\
&= 1 - G^S_{\lambda\lambda}(\delta\lambda)^2 + O((\delta\lambda)^3) \\
&= \frac{1}{\sqrt{Z_W(\beta,\lambda)Z_W(\beta,\delta\lambda)}}|\mathrm{Tr}\Big[e^{-\beta H^\lambda_L} W^{\lambda+\delta\lambda}(-t_w)W^\lambda(-t_w)\Big]|. \qquad (146)
\end{aligned}$$

$G^S_{\lambda\lambda}$ can be explicitly written as

$$\begin{aligned}
G^S_{\lambda\lambda} = \quad & \mathrm{Re}\Big[\ \frac{1}{2}\int_0^{t_w} dt_1 dt_2 \mathrm{Tr}\Big[\frac{e^{-\beta H}}{Z_W(\beta,\lambda)}\Big[W(-t_w),\ V(-t_1)\Big]\cdot\Big[W(-t_w),\ V(-t_2)\Big]^\dagger\Big]\ \Big] \\
& -\frac{1}{2}(\int_0^{t_w} dt \mathrm{Tr}\Big[\frac{e^{-\beta H}}{Z_W(\beta,\lambda)}\Big[W(-t_w),\ V(-t)\Big]\ W(-t_w)\Big])^2. \qquad (147)
\end{aligned}$$

Compared to (139), this quantity does not include constant divergent terms, but only contains terms proportional to commutators of operators. Therefore, we can use this quantity to measure the growth of commutators, therefore scrambling.

4.2 Holographic calculation

In this section, we will show fidelity susceptibility grows rapidly in holographic systems, using proposed holographic dual of fidelity susceptibility. This result is consistent with the prediction from the previous section.

The metric of $d+1$ eternal black hole is given by

$$ds^2 = -f(r)dt^2 + f(r)^{-1}dr^2 + r^2 d\Omega^2_{S^{d-1}}, \qquad (148)$$

where $f(r)$ is given by $r^2 - R^2$ for $d = 2$ with $R^2 = 8G_N M$, and $r^2 + 1 - a^2/r^{d-2}$ for higher dimensions with $a^2 = \frac{G_N M}{\mathrm{Vol}(S^{d-1})}$. R is radius of black hole horizon, and the AdS radius is set to 1. The inverse Hawking temperature β of this black hole is given by $\beta = \frac{4\pi}{f'(R)}$. In the Kruskal coordinate, the metric is written as

$$ds^2 = -\frac{f(r)}{f'(R)^2}e^{-f'(R)r_*(r)}dudv + r^2 d\Omega^2_{S^{d-1}}, \qquad (149)$$

where u and v are given by

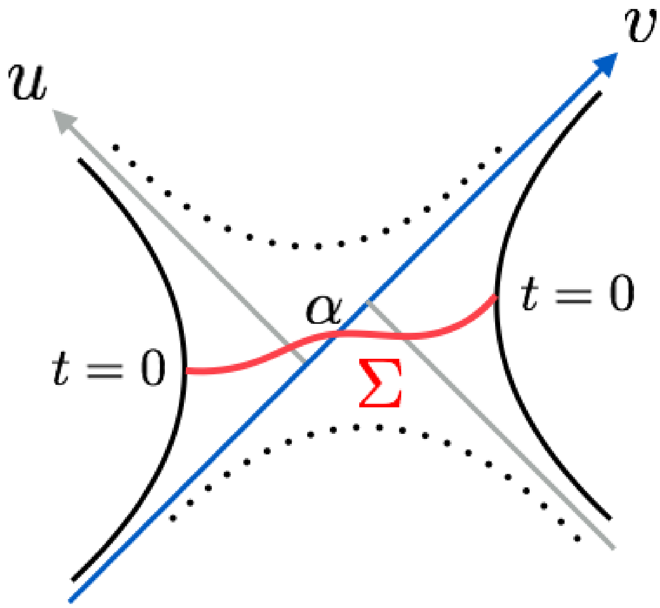

Figure 10: A diagram of the shock wave geometry. Black line are boundaries, dashed lines are singularities, and a blue line is the shock wave. Red surface connecting two boundaries is the extremal volume surface Σ. For 2d CFT, this surface can be understood as configuration of world sheet of a string ending on both boundaries.

$$
\begin{aligned}
u^2 &= e^{f'(R)(r_*(r)-t)} \\
v^2 &= e^{f'(R)(r_*(r)+t)}.
\end{aligned}
\tag{150}
$$

and $r_*(r)$ is defined to satisfy $dr_* = f(r)^{-1}dr$ and $r_*(0) = r_*(\infty) = 0$. The state dual to eternal black hole at $t = 0$ is thermofield double state [21]. We consider a few particles with total energy E are thrown homogeneously into the eternal black hole at $t = -t_w$ from left boundary of the eternal black hole. The proper energy of the particles at $t = 0$ slice is $E_p \approx \frac{E}{R}e^{\frac{2\pi}{\beta}t_w}$. So when t_w is sufficiently large, the particle becomes shock wave, and the geometry can be approximated by shock wave, which is further approximated by glueing two black holes with mass M and mass $M + E$, as shown in fig (10). It is given by $u_L = u_R$ and $v_L = v_R + \alpha$, where α is defined by

$$
\alpha = \frac{E}{u_w}\frac{dR}{dM}C(R, R) \tag{151}
$$

with black hole mass M and $C(r,R) = \frac{e^{f'(R)r_*(r)}}{r-R}$. In 2d, α is given by $\alpha = \frac{E}{4M}e^{\frac{2\pi}{\beta}t_w}$. In higher dimensions, α is proportional to $G_N \cdot E \cdot e^{\frac{2\pi}{\beta}t_w}$.

According to the proposal in [29], fidelity susceptibility of TFD states for exactly marginal deformation is holographically given by the volume of codimension 1 maximal volume surface Σ, which connects $t=0$ slices at two boundaries of spacetimes. This is given as

$$|\langle\Psi_{TFD}(t,\lambda+\delta\lambda)|\Psi_{TFD}(t,\lambda)\rangle| = e^{-n_d(\delta\lambda)^2\mathrm{Vol}(\Sigma)}, \tag{152}$$

where n_d is $\mathcal{O}(1)$ constant. The fidelity susceptibility is then

$$G_{\lambda\lambda} = n_d\mathrm{Vol}(\Sigma). \tag{153}$$

The idea of this proposal stems from Janus geometry [39][40] and the proposed duality between AdS/CFT and MERA [87][88]. The volume of Σ is UV divergent, and we use the radial cutoff in AdS to regularize this volume.

Let's insert a homogeneous scalar operator W on left boundary at $t=-t_w$ and consider the perturbed TFD state at $t=0$. The resulting holographic geometry is approximated by the shock wave geometry for large t_w. The volume of the surface connecting two boundaries at $t=0$ is

$$\mathrm{Vol}(\Sigma) = \int dt d\Omega_{d-1}\sqrt{(-f+\dot{r}^2f^{-1})r^{2(d-1)}}. \tag{154}$$

where $\dot{r} = \frac{dr}{dt}$. When the surface has maximal volume, the conserved quantity along the surface is

$$s_d = \frac{f(r)r^{d-1}}{\sqrt{-f(r)+\dot{r}^2f(r)^{-1}}}. \tag{155}$$

Therefore we conclude that the volume of maximal volume surface is

$$\mathrm{Vol}(\Sigma) = \mathrm{Vol}(S^{d-1})\int drr^{d-1}\sqrt{f(r)^{-1}(1-\frac{1}{1+\frac{f(r)r^{2(d-1)}}{s_d^2}})}. \tag{156}$$

Let us define r_0 by $\dot{r}(r)=0$ and corresponding time as t_0. Then we can express α in terms of s_d as

$$\log\frac{\alpha}{2} = r_*(r_0) + t_0 + \int_{r_0}^{R} dt\frac{1}{|f(r)|\sqrt{1+\frac{f(r)r^{2(d-1)}}{s_d^2}}}(1-\sqrt{1+\frac{f(r)r^{2(d-1)}}{s_d^2}}). \tag{157}$$

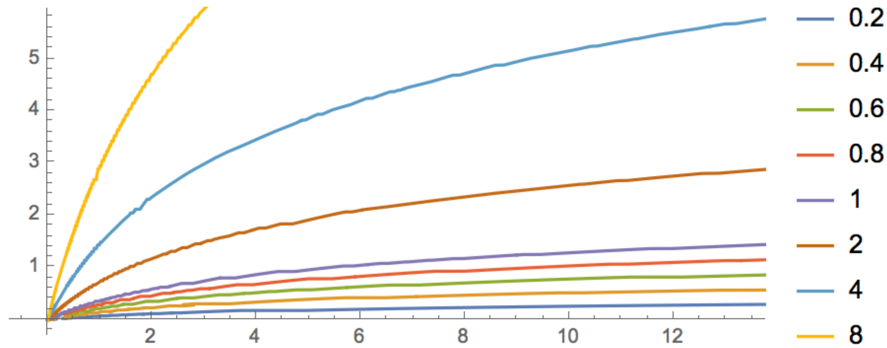

Figure 11: Numerical plot for growth of information metric versus $\alpha = \frac{E}{4M}e^{\frac{2\pi}{\beta}t_w}$ in AdS_3/CFT_2. The numbers in the right are radiuses of BH horizon $R = \frac{2\pi}{\beta}$.The vertical ax is for $2\Delta\mathrm{Vol}$, and horizontal ax is for α.

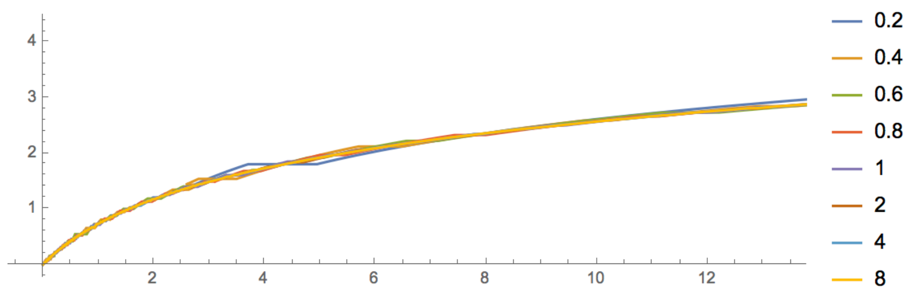

Figure 12: Numerical plot for growth of information metric versus $\alpha = \frac{E}{4M}e^{\frac{2\pi}{\beta}t_w}$ in AdS_3/CFT_2. The numbers in the right are radiuses of BH horizon $R = \frac{2\pi}{\beta}$.The vertical ax is for $\frac{2\Delta\mathrm{Vol}}{R}$, and horizontal ax is for α. We can confirm linear growth of information $\Delta\mathrm{Vol} = f_0 \times R\alpha + \mathcal{O}(\alpha^2)$ for small α, where f_0 does not depend on R.

The numerical result is shown in fig (12), and we can conclude that for $d = 2$,

$$G^{W:c}_{\lambda\lambda} = f_0 \cdot R\alpha + \mathcal{O}(\alpha^2). \tag{158}$$

where f_0 is N and R independent and positive, and indeed it is given by $f_0 \approx 1$. This implies that the fidelity susceptibility for perturbed TFD states for external fields grows exponentially rapidly, proportional to α. This is completely consistent with the perturbative field theory prediction.

4.3 Wilson loop

We can study two point functions of Wilson loops, one Wilson loop on left boundary and the other Wilson loop on another boundary, using holography as was proposed by [89] [90]. We assume these loops are put on the great circles of S^{d-1} on different boundaries. It is expected that such two point functions should decay exponentially in time from the viewpoint of scrambling. In 2d CFT, the two point function is given by Nambu-Goto action

$$\langle W_L W_R \rangle \sim e^{-(S_{NG}-reg)}. \tag{159}$$

Extremal value of Numbu-Goto action is

$$\begin{aligned} S_{NG} &= \frac{1}{2\pi\alpha'}\int dtd\Omega_1\sqrt{(-f+\dot{r}^2 f^{-1})r^2} \\ &= \frac{1}{2\pi\alpha'}\mathrm{Vol}(S^1)\int dr\ r\sqrt{f(r)^{-1}(1-\frac{1}{1+\frac{f(r)r^2}{s_2^2}})}. \end{aligned} \tag{160}$$

This result is same as the calculation of volume of extremal codimension 1 surface, up to constant factor. Therefore, two point function of Wilson loops decays as $\sim f_0 - f_1 \times \alpha + \cdots$ for small α with positive $f_1,\ f_2$, as expected.

In this section, we estimated the time evolution of fidelity susceptibility of thermofield double state perturbed by an operator W at $t = -t_w$. In large N theories, fidelity susceptibility can be separated into two terms, one is unperturbed fidelity susceptibility, and the other is proportional to commutator of V and $W(-t_w)$. Rapid growth of the later term indicates scrambling of W, and sensitivity of time evolution of thermofield double state or thermal mixed states to external environment or internal imperfections. Indeed, we calculated the fidelity susceptibility and confirmed its rapid growth proportional to $e^{\frac{2\pi t}{\beta}}$. This implies that decay of OTO correlator can be understood by growth of distance between different thermal states. We also studied two point function of Wilson loops and confirmed that it decays exponentially.

5 Non Local Deformation, Averaged Null Energy and Quantum Entanglement

Recent study has revealed that non local multi trace deformation renders non traversable wormhole traversable[91]. Wormhole considered in that study is two sided black hole, which has two asymptotically AdS regions. In AdS/CFT, this geometry is dual to thermofield double state on tensor product $\mathrm{CFT}_L \otimes \mathrm{CFT}_R$, and each AdS boundary corresponds to one factor CFT. The non local multi trace deformation added to the CFT action is

$$g \int dt\ d^d x\ h(t,x) \mathcal{O}_L(t,x) \mathcal{O}_R(-t,x), \tag{161}$$

where operator $\mathcal{O}_{L/R}$ is on $CFT_{L/R}$. Such deformation causes null shockwave in the geometry, whose null energy can be positive or negative according to the sign of coupling g. When the averaged null energy is negative, it was found that non traversable wormhole becomes non traversable, even if g is infinitesimally small. Applications and generalizations of such non local multi trace deformations includes, an interpretation as quantum teleportation[92], exploration into black hole interior[93][94], and realization of eternal wormhole[95].

Traversability of wormhole is intimately related to violation of averaged null energy condition (ANEC). Averaged null energy condition is a conjecture, that states integral of null energy on null ray via Affine parameter must be non-negative in any UV complete QFT. ANEC was proved on Minkowski spacetime and other special cases[96][97][98] and its generalization QNEC[99][100][101][102] was also proved on Minkowski space. Averaged null energy has a simple intuitive interpretation, that it measures the change of causal structure, when we perturb solution of vacuum Einstein equation by matter stress tensor. When ANE is negative, null ray in unperturbed metric can become timelike in perturbed metric. Related to this fact, it is known that in classical general relativity, existence of traversable wormhole implies negative ANE. The results of [91][92] are consistent with ANEC of QFT, since once one introduces non local multi trace deformation to the theory, the theory is no longer QFT nor Lorentz invariant, although it is still unitary .

Interesting generalization of previous studies on non local trace deformation is to consider deformation composed of HKLL bulk local operators[103], not just the local operators of boundary CFT. With such deformation, one can manipulate AdS bulk geometry directly, not indirectly through AdS boundary. In other words, one can create bulk local objects which are connected by quantum entanglement. Double trace deformation can be obtained effectively when we integrate out fields which are not relevant to the energy scale under consideration, similar to Van der Waals force[104]. Study on bulk local double trace deformation may help realizing traversable wormhole in pure AdS, or to understand non local effects of higher derivative interactions in string theory.

In order to understand non local multi trace deformations in more detail, it is also important and interesting to study time evolution of field theory observables. In particular, it is important to understand the dynamics of entanglement entropy and entanglement Renyi entropy, with non local multi trace deformation.

In this section, we study time evolution of bulk AdS and boundary CFT, after non local double trace deformation, based on [31]. We focus on non local double trace deformation composed of boundary local operators, as well as HKLL bulk local operators. In both cases, we confirm that with appropriate choice of sign of g, we obtain negative averaged null energy in the bulk. This implies time advance in the bulk, meaning originally light-like separated pair of points becomes time like separated after incorporating the effects of the deformation. Further, we confirm that HKLL bulk local double trace deformation can act as point like source of negative null energy. We then study time evolution of generic CFT_2 after non local double trace deformation, by computing leading correction to entanglement entropy and entanglement Renyi entropy. We found that the leading correction is universal, in other words it depends only on conformal dimension of double trace deformation. Their time dependence shows interesting behavior, as will be described.

First, I will review (achronal) averaged null energy condition, and see how double trace deformation introduced in two sided black hole system, breaks this condition and makes non-traversable wormhole traversable, based on [91].

Then, we consider pure AdS and introduce non local double trace deformation which connects antipodal points in the boundary CFT. We will follow the time evolution after the quench by the double trace deformation, focusing on null energy in the bulk. We confirmed that averaged null energy on null geodesic in the bulk is linear in g, so in particular it can be negative.

Then we consider new type of double trace deformation, composed of HKLL bulk local operators. Such deformation introduces direct quantum correlation between two distinct bulk points. The motivation is to study traversable wormholes in spacetimes with single asymptotic region using AdS/CFT. We then study the spacetime structure after the deformation, in particular null energy in the bulk. We found that, as in the case of section 2, averaged null energy on null geodesic is linear in g so in particular it can be negative.

Finally, we consider time evolution of entanglement entropy and entanglement Renyi entropy after double trace deformation. To calculate entanglement entropy, we use known expression of modular Hamiltonian. And for Renyi entropy, we use Replica trick. In both cases, the leading corrections from the double trace deformation to vacuum are proportional to g. This means one can increase or decrease the entanglement of subsystems by double trace deformation.

5.1 Achronal Averaged Null Energy Condition

Averaged null energy condition is an energy condition, which was shown to be true in any local quantum field theory on flat Minkowski space. The statement is, for any complete null geodesic γ with Affine parameter λ, we have

$$\int d\lambda \langle T_{\mu\nu}\rangle \frac{dx^\mu}{d\lambda}\frac{dx^\nu}{d\lambda} \geq 0. \tag{162}$$

In other words, averaged null energy is always non negative. The statement is weaker than null energy condition, which says we always have

$$\langle T_{\lambda\lambda}\rangle \geq 0 \tag{163}$$

for every null direction λ. Null energy condition is the basis of number of theorems in general relativity, including focussing theorem, singularity theorem, and so on. However, it is known null energy condition can be violated by the existence of matter. But its integrated version, averaged null energy condition, is true on flat spacetime.

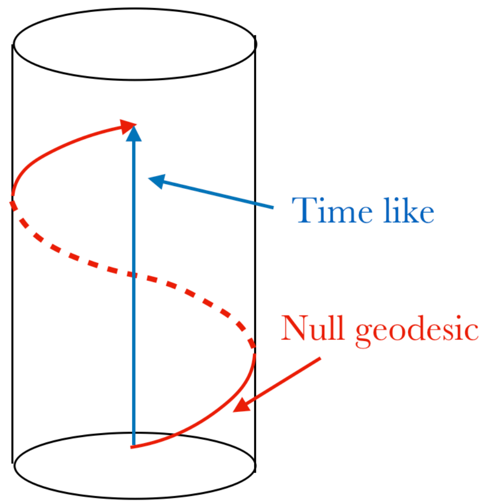

Figure 13: Geodesics on cylinder. Pairs of points on null geodesic (red line) can be connected by time like geodesic (blue line). Therefore, null geodesic is not the boundary of causal future.

On the other hand, when we depart from flat Minkowski space, it is easy to find counterexamples against Averaged Null Energy condition. For example, if we take cylinder, because of Casimir energy. One characteristic of null geodesic in cylinder is that null geodesic is not the boundary of causal future. In other words, there are pairs of points on each null geodesic, which can be connected via time like geodesic. A possible cure of this problem is to impose a condition on null geodesic, namely, we require null geodesic to be achronal. Achronal null geodesic is null geodesic, on which any pair of points can not be connected via time like geodesic. This requirement exclude, for example, null geodesics on cylinder. This condition is called Achronal Averaged Null Energy Condition.

5.2 Double trace deformation in two sided black hole

In this section, I will review how double trace deformation renders non traversable wormhole in two sided black hole to be traversable. We consider double trace deformation of the form

$$S = \int dx \int dt h(t,\ x)\mathcal{O}^L(t,\ x)\mathcal{O}^R(t,\ x), \tag{164}$$

where $h(t,\ x)$ has support only after turning on time t_0. Note that we took the time convention in such a way that arrows of time are the same for both boundaries. With such deformation, it was found that non traversable wormhole in two sided black hole, can become traversable.

Indeed, such deformation introduces non trivial bulk stress tensor expectation values, and its leading term is proportional to h. This implies that with appropriate sign of h, null energy

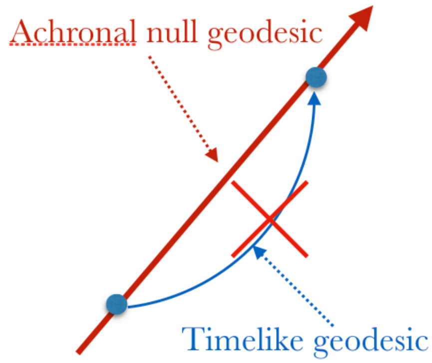

Figure 14: Description of achronal null geodesic. No time like geodesic can connects a pair of points on achronal null geodesic.

and averaged null energy can be negative, as long as the linear term does not vanish. One can indeed confirm that such linear term does not vanish.

In the case of two sided black hole, averaged null energy on the null geodesic $U = 0$ is directly related to the traversablity of the wormhole. Let us consider null ray of deformed geometry embedded in undeformed geometry. We assume it initially coincide with black hole horizon. We regards U coordinate value of this embedded null geodesic as function of $-1 \leq V \leq 1$. On this null geodesic, we have

$$\int_{-1}^{V} dV T_{VV} = \frac{1}{8\pi G_N}\frac{1}{2}(-2g_{UV}(0))R_{AdS}^{-2} \cdot U(V), \tag{165}$$

where $g_{UV}(0) = -1$ is the UV component of undeformed metric at $U = 0$ which is negative, and R_{AdS} is the AdS radius. This equation implies that when averaged null energy is negative, we have negative $U(1)$. This implies that the originally non-traversable wormhole is rendered to be traversable, via non local double trace deformation.

5.3 Double trace deformation of boundary local operators

In this section, we consider time evolution of bulk after introducing non local double trace deformation. We consider holographic CFT dual to classical gravity on pure global AdS_3

$$ds^2 = \frac{1}{\cos^2\rho}(-d\tau^2 + d\rho^2 + \sin^2\rho d\theta^2), \tag{166}$$

where $0 \leq \rho \leq \frac{\pi}{2}$, $-\pi < \theta < \pi$ and $-\infty < \tau < \infty$.
We deform CFT Hamiltonian by non local double trace deformation

$$H \to H^g(t) := H + g\mathcal{O}(0,0)\mathcal{O}(0,\pi)f(t), \tag{167}$$

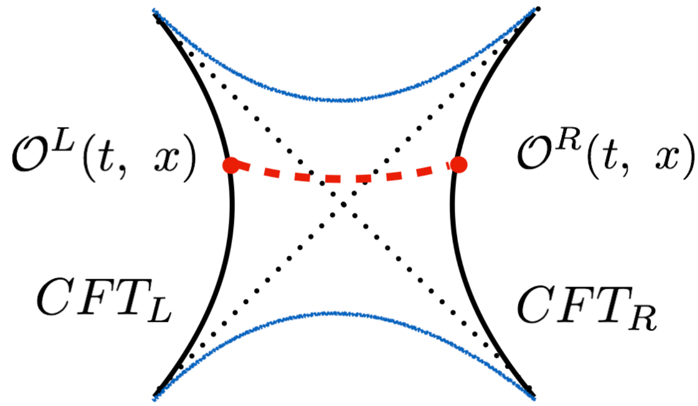

Figure 15: Double trace deformation in two sided black hole.

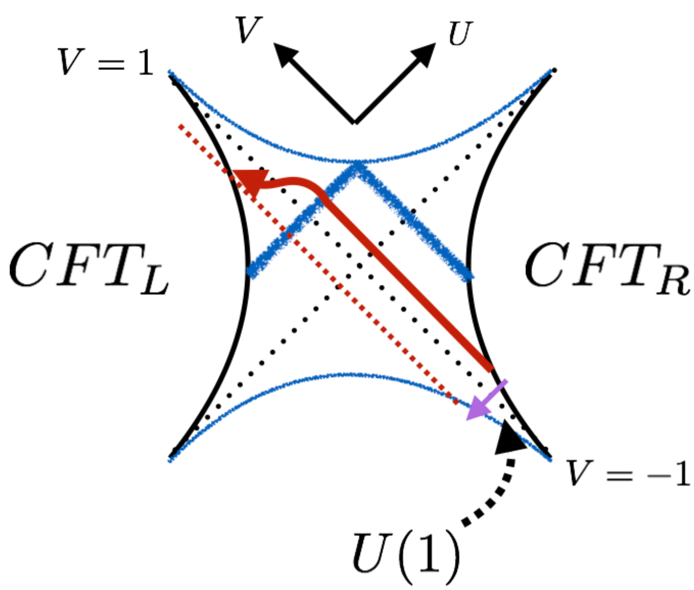

Figure 16: We embed null geodesic of deformed geometry into undeformed geometry, starting at boundary point $V=-1$(red line). Because of double trace deformation and violation of ANEC, the null geodesic looks like space like in undeformed geometry, and can reach another boundary at some point. This implies the originally non traversable wormhole turns into traversable wormhole.

which is designed to connect two distinct points $\theta = 0$ and $\theta = \pi$ at the AdS boundary. $\mathcal{O}$ is scalar primary operator of the CFT with conformal dimension $\Delta = \delta + \bar{\delta}$. And g is a deformation parameter, infinitesimally small, and $f(t)$ is some real function that only depends on t. In most of the cases I will assume $f(t) = \delta(t)$.

Such non local double trace deformation does not produce non zero scalar fields at the linear order in g, but does produce nontrivial configuration of matter stress tensor in the bulk, which we will study below. From now on, we assume CFT central charge is large, so that the bulk gravity is classical Einstein gravity. We also ignore the back reaction to gravity from matter fields.

We first compute perturbed bulk two point function, using HKLL bulk local operator. HKLL bulk local operator is a CFT operator, which can be interpreted as a bulk local field in the following way. Two point function of HKLL bulk local operators for massive scalar in AdS is

$$(\nabla^2_{AdS_3} - M^2)\langle\Phi(t,\rho,\theta)\Phi(t',\rho',\theta')\rangle = \frac{1}{\sqrt{-g^{(3)}}}\delta^3((t,\rho,\theta),(t',\rho',\theta')) \tag{168}$$

with boundary condition

$$\frac{1}{(\cos\rho)^{\Delta}}\Phi(t,\rho,\theta) \underset{\rho\to\frac{\pi}{2}}{\to} \mathcal{O}(t,\theta). \tag{169}$$

where $M^2 = \Delta(\Delta-2)$.

Let us first consider time evolution of HKLL bulk local operator. After deformation, it is given by

$$\begin{aligned}\Phi^g(t,\rho,\theta) \quad &= \tilde{P}e^{i\int_{-\infty}^{t} d\tilde{t}\ e^{iH\tilde{t}}(H^g(\tilde{t})-H)e^{-iH\tilde{t}}}\Phi(t,\rho,\theta)Pe^{-i\int_{-\infty}^{t} d\tilde{t}\ e^{iH\tilde{t}}(H^g(\tilde{t})-H)e^{-iH\tilde{t}}} \\ &= \Phi(t,\rho,\theta) + i\int_{-\infty}^{t} d\tilde{t}\ [e^{iH\tilde{t}}(H^g(\tilde{t})-H)e^{-iH\tilde{t}},\ \Phi(t,\rho,\theta)] + \mathcal{O}(g^2).\end{aligned} \tag{170}$$

Then the first order change of bulk two point function is given by

$$\begin{aligned}&\langle\Phi^g(t,\rho,\theta)\Phi^g(t',\rho',\theta')\rangle - \langle\Phi(t,\rho,\theta)\Phi(t',\rho',\theta')\rangle \\ &= ig\int_{-\infty}^{t} d\tilde{t}\ f(\tilde{t})\langle[\mathcal{O}(\tilde{t},0)\mathcal{O}(\tilde{t},\pi),\Phi(t,\rho,\theta)]\Phi(t',\rho',\theta')\rangle + c.c_{(t,\rho,\theta)\leftrightarrow(t',\rho',\theta')} + \mathcal{O}(g^2) \\ &\approx ig\int_{-\infty}^{t} d\tilde{t}\ f(\tilde{t})\Big(\langle[\mathcal{O}(\tilde{t},0),\Phi(t,\rho,\theta)]\rangle\langle\mathcal{O}(\tilde{t},\pi)\Phi(t',\rho',\theta')\rangle \\ &+\langle[\mathcal{O}(\tilde{t},\pi),\Phi(t,\rho,\theta)]\rangle\langle\mathcal{O}(\tilde{t},0)\Phi(t',\rho',\theta')\rangle\Big) + c.c_{(t,\rho,\theta)\leftrightarrow(t',\rho',\theta')} + \mathcal{O}(g^2)\end{aligned} \tag{171}$$

In the final line I used large N approximation.

Once we know bulk two point function, we can compute expectation value of bulk stress tensor perturbatively. The bulk energy momentum tensor is

$$T_{\mu\nu} = \partial_\mu \phi \partial_\nu \phi - \frac{1}{2} g_{\mu\nu} g^{\rho\sigma} \partial_\rho \phi \partial_\sigma \phi - \frac{1}{2} g_{\mu\nu} M^2 \phi^2, \tag{172}$$

so the expectation value of stress tensor can be obtained by point splitting method with coincident point divergence subtracted, as follows,

$$\langle T_{\mu\nu} \rangle = \operatorname*{Lim}_{x \to x'} \Big(\partial_\mu \partial'_\nu G(x,x') - \frac{1}{2} g_{\mu\nu} g^{\rho\sigma} \partial_\rho \partial'_\sigma G(x,x') - \frac{1}{2} g_{\mu\nu} M^2 G(x,x') \Big), \tag{173}$$

where $G(x,x') := \langle \Phi(x) \Phi(x') \rangle$.

Before obtaining actual values. let us summarize the propagators in global AdS_3. First we define

$$z = \frac{\cos(t-t') - \sin\rho \sin\rho' \cos(\theta - \theta')}{\cos\rho \cos\rho'} \tag{174}$$

The bulk two point function scalar of mass $m^2 = \Delta(\Delta - 2)$ for space-like configuration is

$$\langle \Phi(t,\rho,\theta) \Phi(t',\rho',\theta') \rangle = \frac{1}{4\pi} (z^2-1)^{-\frac{1}{2}} (z + (z^2-1)^{\frac{1}{2}})^{1-\Delta} \tag{175}$$

In order to continue to time-like configuration, we need a shift ($\epsilon > 0$)

$$t \to t - i\epsilon \tag{176}$$

since we are dealing with Wightman function, not time-ordered propagator which requires $t \to t(1 - i\epsilon)$. In Wightman case we have

$$z \to z + i \, \frac{\sin(t-t')}{\cos\rho \cos\rho'} \epsilon. \tag{177}$$

So the full expression of Wightman function is

$$\langle \Phi(t,\rho,\theta) \Phi(t',\rho',\theta') \rangle = \theta(z-1) \frac{e^{-\frac{in\pi}{2}}}{4\pi} (z^2-1)^{-\frac{1}{2}} (z + e^{\frac{in\pi}{2}} (z^2-1)^{\frac{1}{2}})^{1-\Delta} \tag{178}$$

where $|n|$ is the number of intersecting points, between geodesic connecting two points and light cone of (t', ρ', ϕ'). And n is positive when $t > t'$, and is negative when $t < t'$.

Then the commutator is

$$\langle[\Phi(t,\rho,\phi),\ \Phi(t',\rho',\phi')]\rangle = 2i\ \mathrm{Im}\langle\Phi(t,\rho,\theta)\Phi(t',\rho',\theta')\rangle \tag{179}$$

The bulk-boundary two point function at spacelike separation is

$$\begin{aligned}
&\langle\Phi(t,\rho,\phi)\mathcal{O}(t',\phi')\rangle\\
&= \underset{\rho'\to\frac{\pi}{2}}{Lim}\frac{1}{cos^{\Delta}\rho'}\langle\Phi(t,\rho,\phi)\Phi(t',\rho',\phi')\rangle\\
&= \frac{1}{2\pi}\Big(\frac{(\cos\rho)/2}{\cos(t-t')-\sin\rho\ \cos(\theta-\theta')+i\ \sin(\mathrm{t}-\mathrm{t}')\epsilon}\Big)^{\Delta}
\end{aligned} \tag{180}$$

So the bulk-boundary two point function is

$$\begin{aligned}
&\langle\Phi(t,\rho,\phi)\mathcal{O}(t',\phi')\rangle\\
&= \frac{1}{2\pi}\Big(|\frac{(\cos\rho)/2}{\cos(t-t')-\sin\rho\ \cos(\theta-\theta')}|\Big)^{\Delta}e^{-in\Delta\pi}.
\end{aligned} \tag{181}$$

$|n|$ is the number of intersecting points, between geodesic connecting two points and light cone of (t',ϕ'). And n is positive when $t>t'$, and is negative when $t<t'$. Therefore the commutator is

$$\langle[\Phi(\tau,\rho,\phi),\ \mathcal{O}(\tau',\phi')]\rangle \qquad = \frac{1}{2\pi}\Big(\frac{\cos\rho/2}{|\cos(t-t')-\sin\rho\ \cos(\theta-\theta')|}\Big)^{\Delta}\ (-2i\sin(n\Delta\pi)) \tag{182}$$

In the computation of averaged null energy, we use naive regularization with infinitesimal positive parameter a as follows. For bulk to boundary propagator, when the separation is spacelike, we use

$$\begin{aligned}
&\langle\Phi(t,\rho,\phi)\mathcal{O}(t',\phi')\rangle\\
&= \frac{1}{2\pi}\Big(\frac{(\cos\rho)/2}{\cos(t-t')-\sin\rho\ \cos(\theta-\theta')+a^2}\Big)^{\Delta}e^{-in\Delta\pi},
\end{aligned} \tag{183}$$

and for timelike separation

$$\begin{aligned}&\langle \Phi(t,\rho,\phi)\mathcal{O}(t',\phi')\rangle \\ &= \frac{1}{2\pi}\Big(\frac{(\cos\rho)/2}{-\cos(t-t')+\sin\rho\ \cos(\theta-\theta')+a^2}\Big)^{\Delta} e^{-in\Delta\pi}.\end{aligned} \tag{184}$$

For the bulk to bulk propagator at spacelike separation, we regularize as

$$\langle \Phi(t,\rho,\theta)\Phi(t',\rho',\theta')\rangle = \frac{e^{-in\pi/2}}{4\pi}(z^2-1+a^2)^{-\frac{1}{2}}(z+e^{in\pi/2}(z^2-1+a^2)^{\frac{1}{2}})^{1-\Delta}, \tag{185}$$

and at timelike separation, we regularize as

$$\langle \Phi(t,\rho,\theta)\Phi(t',\rho',\theta')\rangle = \frac{e^{-in\pi/2}}{4\pi}(-z^2+1+a^2)^{-\frac{1}{2}}(z+e^{in\pi/2}(-z^2+1+a^2)^{\frac{1}{2}})^{1-\Delta}. \tag{186}$$

Let us assume $f(t)=\delta(t)$, so that the double trace deformation is instantaneous. Then we can obtain analytical expression for bulk stress tensors, using known expression of bulk two point function. In order to explore dynamics of bulk matter, we will focus on $\langle T_{tt}\rangle$ and null energy in the bulk and averaged null energy on null geodesics.

Averaged null energy is defined by an integral of null energy on complete null geodesic via affine parameter. I will consider null geodesics passing through the center of global AdS_3 as well as the spacetime points where we put the deformation. The null geodesic starts at $t=t_0$ and $\theta=\theta_0+\pi$, and ends at $t=t_0+\pi$ and $\theta=\theta_0$.

$$\rho = -\mathrm{Arctan}(\lambda),\quad t=-\rho+t_0+\frac{\pi}{2},\quad \theta=\theta_0+\pi \tag{187}$$

for $\lambda<0$ and

$$\rho = \mathrm{Arctan}(\lambda),\quad t=\rho+t_0+\frac{\pi}{2},\quad \theta=\theta_0 \tag{188}$$

for $\lambda>0$, where λ is an affine parameter.

Let's compute Null energy on those null geodesics

$$\langle T_{\lambda\lambda}\rangle = \langle T_{\mu\nu}\rangle\frac{dx^{\mu}}{d\lambda}\frac{dx^{\nu}}{d\lambda} = \frac{\langle T_{tt}+2\mathrm{sign}(\lambda)T_{t\rho}+T_{\rho\rho}\rangle}{(1+\lambda^2)^2}. \tag{189}$$

We can compute right hand side of this formula by point splitting,

$$\langle T_{tt}+2\mathrm{sign}(\lambda)T_{t\rho}+T_{\rho\rho}\rangle = \operatorname*{Lim}_{x\to x'}(\partial_\rho\partial_{\rho'}+\mathrm{sign}(\lambda)(\partial_\rho\partial_{t'}+\partial_{\rho'}\partial_t)+\partial_t\partial_{t'})G(x,x'). \tag{190}$$

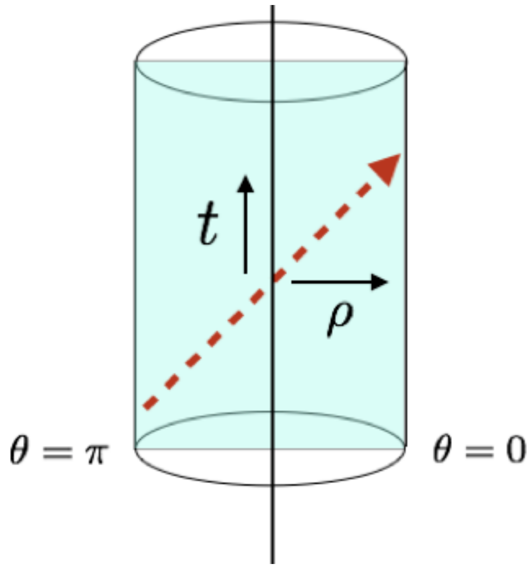

Figure 17: The geometry of global AdS_3. Red line is null ray, on which we compute averaged null energy. On blue plane we compute null energy, and null direction is set as that of the red line.

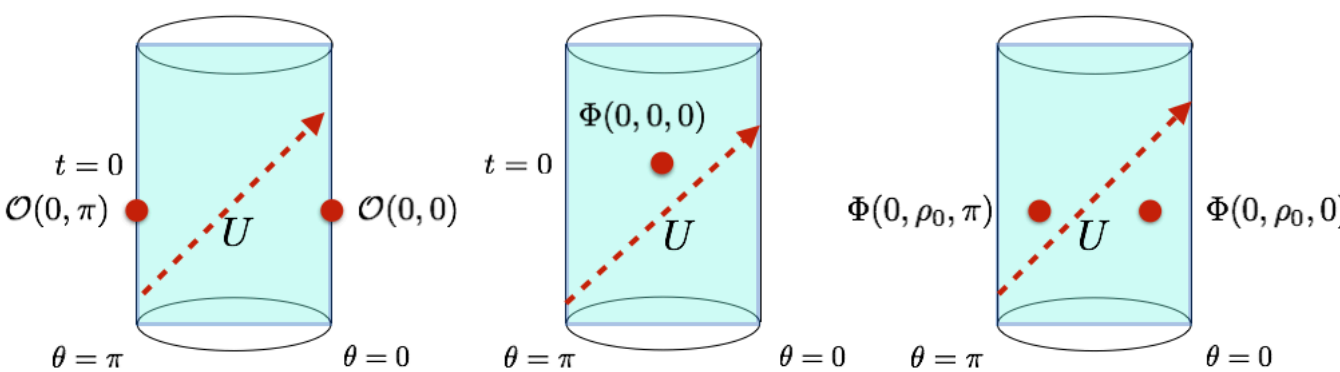

Figure 18: The configurations of double trace deformations we consider in this thesis. (Left) Double trace deformation composed of boundary local operator.(Center) Single trace deformation in the bulk. (Right) Double trace deformation pushed into the bulk.

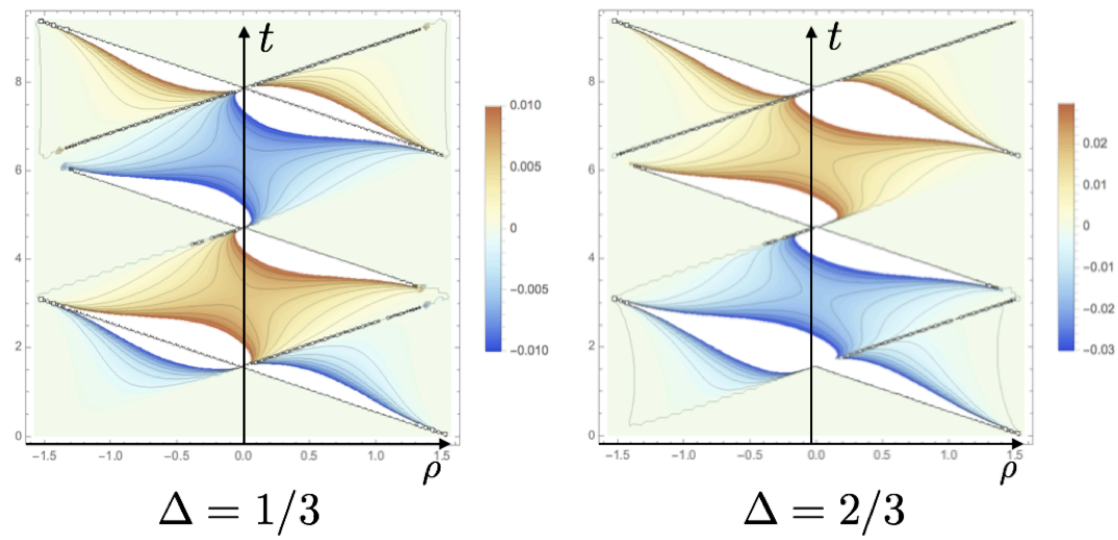

Figure 19: Plots of null energy $T_{\lambda\lambda}$ in the bulk on $\theta = 0$ (and $= \pi$) plane. U is taken to be θ growing direction. We can observe non zero null energy is emitted from the two points where we inserted double trace deformation. Note that on any null geodesic incoming from $\theta = \pi$ and $-\pi < \theta < 0$, null energy is negative, when g is positive. This result is Δ independent.

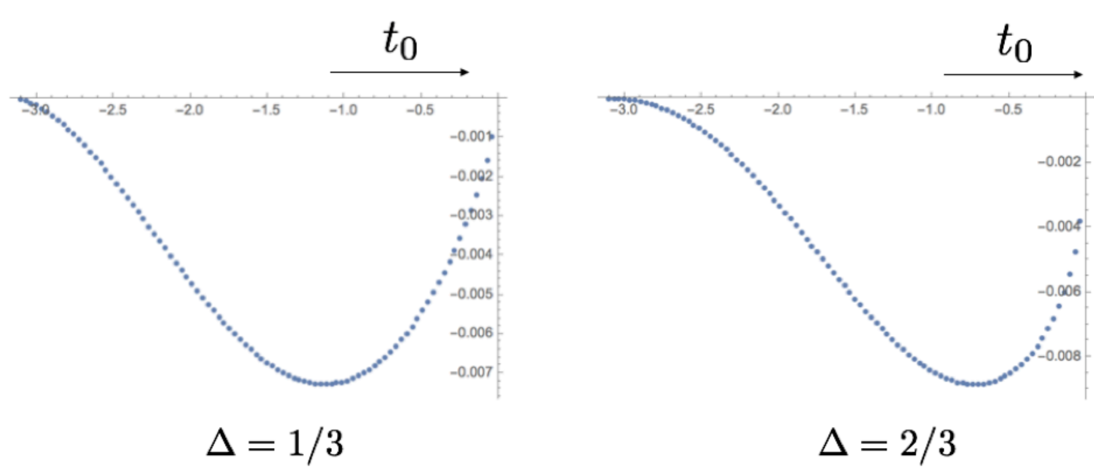

Figure 20: Plots of Averaged null energies on null geodesics when the theory is deformed by boundary double trace deformation. The null geodesic starts at boundary of AdS with $\theta = \pi$ and $t = t_0$, then ends at AdS boundary with $\theta = 0$ and $t = t_o + \pi$. Averaged null energy is divergent and we regularized it using a defined in appendix A. The averaged null energy is proportional to $\frac{g}{a^{2\Delta}}$ and the plot is describing the coefficient of $\frac{g}{a^{2\Delta}}$. Note that on any null geodesic incoming from $\theta = \pi$ and $-\pi < \theta < 0$, null energy is negative, when g is positive. This behavior is Δ independent.

Let us assume $f(t) = \delta(t)$ and $\theta_0 = 0$. We plot null energy $\langle T_{\lambda\lambda} \rangle$ and averaged null energy $\int d\lambda \langle T_{\lambda\lambda} \rangle$.

We can confirm that when the sign of g is positive, averaged null Energy is negative for $-\pi < t_0 < 0$ for any Δ. So the null ray emitted into bulk in this period gets time shift, and becomes time like after incorporating matter stress tensor contributions in Einstein equation. In general relativity where we usually assume averaged null energy conditions, we usually have time delay, meaning light ray going through gravitating region always delays compared to light ray passing through flat region at asymptotic infinity[106][107]. Similar statement for asymptotically AdS spacetime also holds[108][109]. Note that the averaged null energy is divergent and is proportional to $g/a^{2\Delta}$, where a is lattice spacing. Naive counting of dimension of g is $1 - 2\Delta$, so averaged null energy has naive dimension 1.

5.4 Double trace deformation by bulk local operators

In this subsection, we consider multi trace deformation using HKLL bulk local operators. Our bulk non local double trace deformation models quantum operation on bulk tensor network, bulk non local interaction, and bulk micro traversable wormhole. The motivation to study such deformation is to construct wormhole inside spacetime with single asymptotically AdS region, unlike two sided black hole with two asymptotically AdS regions. Time evolutions of bulk matter and spacetime after introduction of bulk local excitations were discussed in [110][111]. In this subsection, we compute time evolution of null energy and averaged null energy, and find that both of them can be negative, so we can have time advance in gravity.

5.4.1 Single trace deformation

To start with, we consider single trace deformation to Hamiltonian by HKLL bulk local operator. Let's assume the bulk local operator put at the center of AdS. The deformation is

$$H \to H + g\Phi_{bulk}(t, 0, 0)f(t) \tag{191}$$

where Φ_{bulk} is HKLL bulk local operator. The vacuum expectation value of bulk local field is then given by

$$\langle \Phi^f(t, \rho, \theta) \rangle = ig \int_{-\infty}^{t} d\tilde{t}\; f(\tilde{t}) \langle [\Phi(\tilde{t}, 0, 0), \Phi(t, \rho, \theta)] \rangle + \mathcal{O}(g^2). \tag{192}$$

We assume $f(t) = \delta(t)$, then we can compute the expectation value of bulk stress energy tensors. The leading term in null energy is proportional to g^2 with positive coefficient as shown in Figure 5. So the null energy is positive everywhere and there are no violations of ANEC in this case.

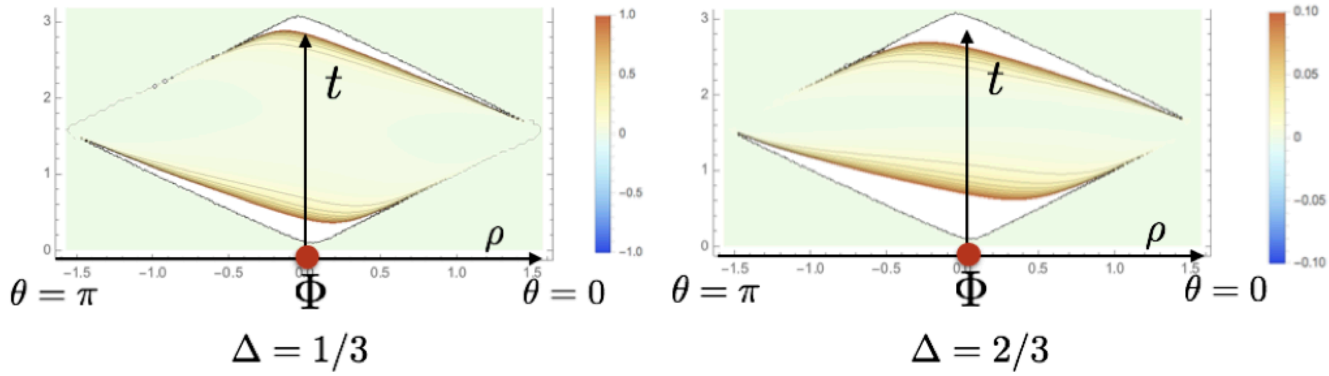

Figure 21: Time evolution of null energy in the case when we introduce single trace deformation in the bulk, divided by g^2. We can observe positive null energy is emitted from the point where we inserted single trace deformation. In particular, null energy is always positive everywhere.

5.5 Double trace deformation

In this subsection, we consider double trace deformation using HKLL bulk local operators, in order to model micro traversable wormhole connecting bulk points. In this case the deformation lives inside bulk, not on AdS boundary.

We consider deformation of Hamiltonian

$$H \to H + g\Phi_{bulk}(t, \rho_0, 0)\Phi_{bulk}(t, \rho_0, \pi)f(t), \tag{193}$$

where Φ_{bulk} is HKLL bulk local operator. The computation of null energy goes in the same way as in the previous section. The perturbed bulk two point function is

$$\begin{aligned}
&\langle \Phi^f(t, \rho, \theta)\Phi^f(t', \rho', \theta')\rangle - \langle \Phi(t, \rho, \psi)\Phi(t', \rho', \theta')\rangle \\
&= ig\int_{-\infty}^{t} d\tilde{t}\ f(\tilde{t})\langle [\Phi(\tilde{t}, \rho_0, 0)\Phi(\tilde{t}, \rho_0, \pi), \Phi(t, \rho, \theta)]\Phi(t', \rho', \theta')\rangle + c.c_{(t,\rho,\theta)\leftrightarrow(t',\rho',\theta')} + \mathcal{O}(g^2) \\
&\approx ig\int_{-\infty}^{t} d\tilde{t}\ f(\tilde{t})\Big(\langle [\Phi(\tilde{t}, \rho_0, 0), \Phi(t, \rho, \theta)]\rangle\langle \Phi(\tilde{t}, \rho_0, \pi)\Phi(t', \rho', \theta')\rangle + (0 \leftrightarrow \pi)\Big) \\
&+c.c_{(t,\rho,\theta)\leftrightarrow(t',\rho',\theta')} + \mathcal{O}(g^2),
\end{aligned} \tag{194}$$

which can be computed by analytical continuation of bulk two point functions[105].

Then, by using point splitting, we can compute null energy and averaged null energy in the bulk. The results are shown in Figures. We confirm that when the sign of g is positive,

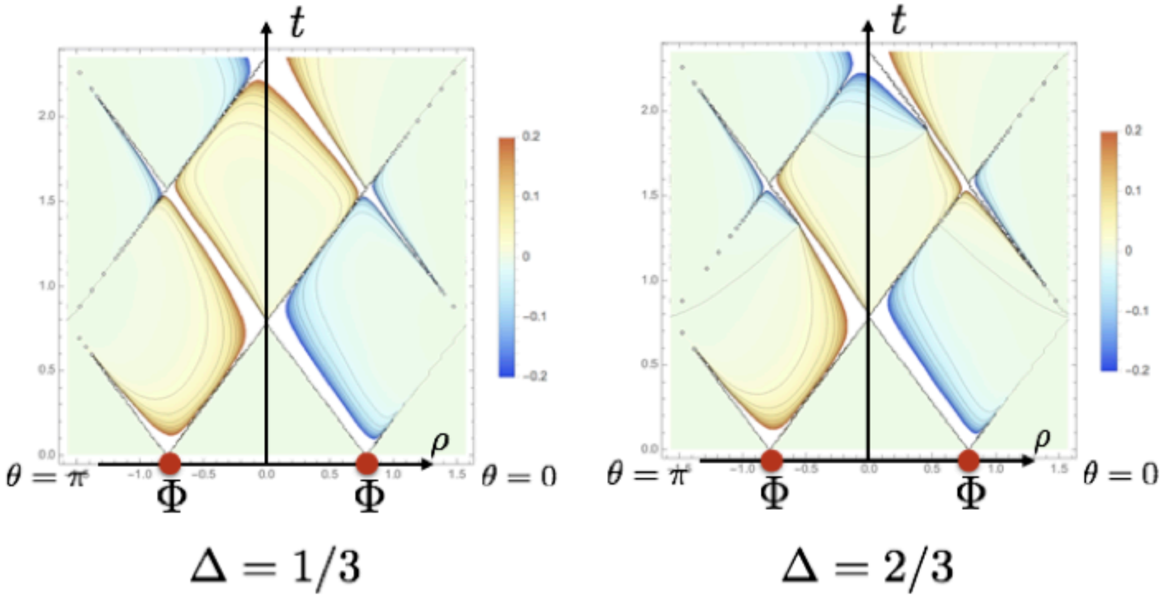

Figure 22: Plots of null energy T_{UU} in the bulk on $\theta = 0$ (and $= \pi$) plane. U is taken to be θ growing direction. We can observe non zero null energy is emitted from the two points where we inserted double trace deformation. Note that on any null geodesic incoming from $\theta = \pi$ and $-\pi < \theta < 0$, null energy is negative, when g is positive. This fact is Δ independent. The left figure is for $\Delta = 1/3$ case, and the right figure is for $\Delta = 2/3$ case.

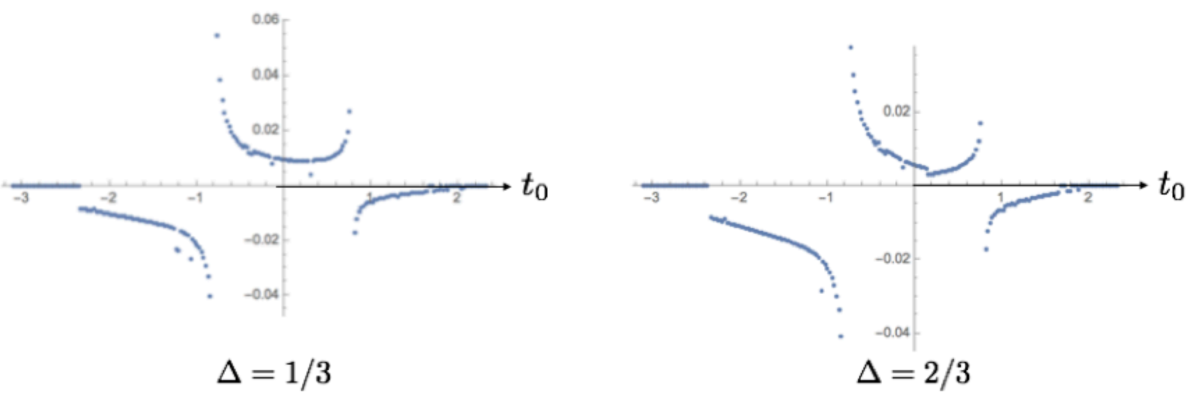

Figure 23: Plots of Averaged null energies on null geodesics when the theory is deformed by bulk double trace deformation. The null geodesic starts at boundary of AdS with $\theta = \pi$ and $t = t_0$, then ends at AdS boundary with $\theta = 0$ and $t = t_o + \pi$. Averaged null energy is divergent and we regularized it using a defined in appendix A. The averaged null energy is proportional to $\frac{g}{a}$ and the plot is describing the coefficient of $\frac{g}{a}$. Note that on any null geodesic incoming from $\theta = \pi$ and $-\pi < \theta < 0$, null energy is negative, when g is positive. This behavior is Δ independent.

averaged null Energy is negative for $-3\pi/4 < t_0 < -\pi/4$ for any Δ. So the null ray emitted into bulk in this period gets time shift and becomes time like after incorporating matter stress tensor in Einstein equation. Note that the averaged null energy is divergent and is proportional to g/a, where a is lattice spacing. Naive counting of dimension of g is 0, so averaged null energy has naive dimension 1.

One can check that when the HKLL operators approach to the boundary, then identical behavior as that of boundary local double trace deformation can be confirmed, as it should be.

5.6 CFT analysis

In this subsection, we consider time evolution of entanglement entropy and Renyi entropy in general two dimensional CFT on Minkowski space. Entanglement entropy has been studied from various viewpoints, including from CFT[112] as well as from AdS/CFT[12]. The setup we will use in this subsection can be regarded as a version of quantum quench[113][114][115][116][117][118] with non local deformation. Perturbative computation of entanglement entropy with time dependent relevant deformation is discussed in [119]. Entanglement entropies of non local theories are discussed in [120][121]. We consider time evolution of vacuum state after acting double trace operation $e^{-ig\mathcal{O}(0)\mathcal{O}(L)}$. The non-reduced, regularized density matrix is given by

$$\begin{aligned} \rho(g,t) \quad &= e^{-iHt}e^{-\epsilon H}e^{-ig\mathcal{O}\mathcal{O}}|0\rangle\langle 0|e^{ig\mathcal{O}\mathcal{O}}e^{-\epsilon H}e^{iHt}/\mathcal{N}_g \\ &= e^{-ig\mathcal{O}\mathcal{O}(-(t-i\epsilon))}|0\rangle\langle 0|e^{ig\mathcal{O}\mathcal{O}(-(t+i\epsilon))}/\mathcal{N}_g, \end{aligned} \tag{195}$$

where $\mathcal{O}(t-i\tau) = e^{H(it+\tau)}\mathcal{O}e^{-H(it+\tau)}$, and ϵ is an infinitesimal positive constant, and $\mathcal{N}_g = \langle 0|e^{ig\mathcal{O}\mathcal{O}}e^{-2\epsilon H}e^{-ig\mathcal{O}\mathcal{O}}|0\rangle = 1 + \mathcal{O}(g^2)$. We will take subregion A as $[x,\infty]$, and consider entanglement structure of the reduced density matrix $\mathrm{Tr}_{\mathcal{H}_{\bar{A}}}\rho(g,t)$.

5.6.1 Entanglement Entropy

Let us first start with time evolution of entanglement entropy of subsystem A. Using modular Hamiltonian $H_A = -\log\rho_A$, entanglement entropy can be expressed as

$$S_A = -\mathrm{Tr}[\rho_A \log\rho_A] = \langle H^A_{mod}\rangle. \tag{196}$$

In the case of vacuum modular Hamiltonian of half space in 2d QFT, modular Hamiltonian can be written explicitly in terms of energy momentum tensor[122], we have

$$H^A_{mod} = 2\pi\int_x^\infty d\tilde{x}\ (\tilde{x}-x)T_{00}(0,\tilde{x}) + Const. \tag{197}$$

Let us consider double trace deformation on CFT ground state in perturbation theory. Perturbation theory of entanglement entropy is discussed in [123][124]. From the normalization condition, we have

$$\mathrm{Tr}_{\mathcal{H}_A}[e^{-H^A_{mod}(t,g)}\frac{d}{dg}H^A_{mod}(t,g)] = 0. \tag{198}$$

Then, the entanglement entropy is given by

$$\begin{aligned} S_A(t,g) \quad &= \mathrm{Tr}_{\mathcal{H}_A}[e^{-H^A_{mod}(t,g)}H^A_{mod}(t,0)] + \mathcal{O}(g^2) = \mathrm{Tr}_{\mathcal{H}}[e^{-H_{mod}(t,g)}(H^A_{mod}(t,0)\otimes 1_{\mathcal{H}_{\bar{A}}})] + \mathcal{O}(g^2) \\ &= S_A(0,0) + ig\Big(\langle\mathcal{O}\mathcal{O}(-(t+i\epsilon))H^A(g=0)\rangle - \langle H^A(g=0)\mathcal{O}\mathcal{O}(-(t-i\epsilon))\rangle\Big) + \mathcal{O}(g^2). \end{aligned} \tag{199}$$

From conformal Ward-Takahashi identity, we have

$$\langle T(z)\mathcal{O}(0,L)\mathcal{O}(0,0)\rangle = \frac{2h}{L^{4h+1}}(-\frac{1}{z-L}+\frac{1}{z}) + \frac{h}{L^{4h}}(\frac{1}{z^2}+\frac{1}{(z-L)^2}). \tag{200}$$

As a result,

$$\begin{aligned} &\Delta S_A = -2\pi i g\int_x^\infty d\tilde{x}\ (\tilde{x}-x) \\ &\Big(\langle\mathcal{O}(-(t+i\epsilon),L)\mathcal{O}(-(t+i\epsilon),0)(T(0,\tilde{x})+\bar{T}(0,\tilde{x}))\rangle \\ &-\langle(T(0,\tilde{x})+\bar{T}(0,\tilde{x}))\mathcal{O}(-(t-i\epsilon),L)\mathcal{O}(-(t-i\epsilon),0)\rangle\Big). \end{aligned} \tag{201}$$

Therefore, one need to evaluate

$$\begin{aligned} &-2\pi i g\int_x^\infty d\tilde{x}\ (\tilde{x}-x)\Big(\frac{2h}{L^{4h+1}}(-\frac{1}{z-L}+\frac{1}{z}) + \frac{h}{L^{4h}}(\frac{1}{z^2}+\frac{1}{(z-L)^2}) \\ &+\frac{2h}{L^{4h+1}}(-\frac{1}{\bar{z}-L}+\frac{1}{\bar{z}}) + \frac{h}{L^{4h}}(\frac{1}{\bar{z}^2}+\frac{1}{(\bar{z}-L)^2})\Big), \end{aligned} \tag{202}$$

with $z = \tilde{x} - (t \pm i\epsilon)$ and $\bar{z} = \tilde{x} + (t \pm i\epsilon)$. The total shift of entanglement entropy is then

$$\begin{aligned} &\Delta S_A = \frac{4\pi^2 gh}{L^{4h}}\Big(\theta(t-x)+\theta(t+L-x)-\theta(-t-x)-\theta(-t+L-x)\Big) - \frac{8\pi^2 gh}{L^{4h+1}} \\ &\times\Big((t+L-x)\theta(t+L-x)-(t-x)\theta(t-x)-(-t+L-x)\theta(-t+L-x)+(-t-x)\theta(-t-x)\Big). \end{aligned} \tag{203}$$

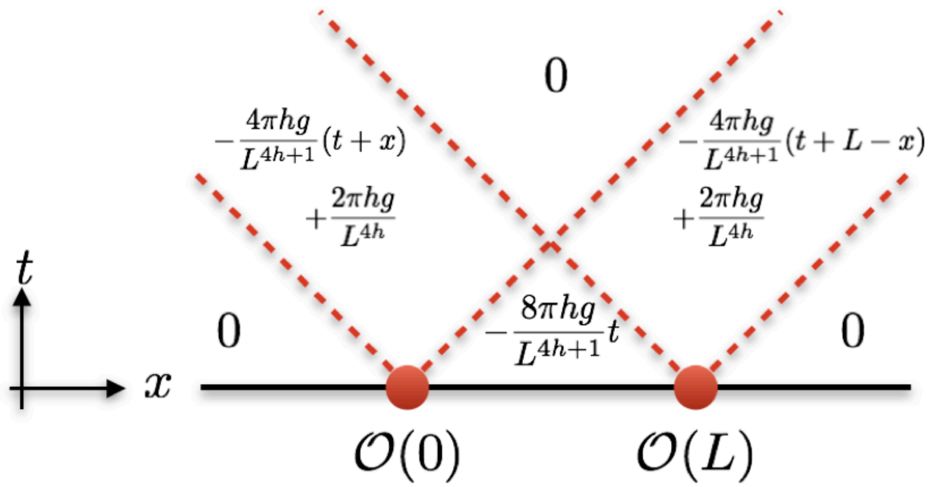

Figure 24: Spacetime dependence of entanglement entropy ΔS_A after double trace deformation. When $x > t + L$ or $x + t < 0$, ΔS_A must be zero from causality.

Interestingly, when $t+x-L > 0$ and $t-x > 0$, we have $\Delta S_A = 0$. The reason why$\Delta S_A = 0$ in $x-t-L > 0$ and $-x+t > 0$ comes from causality. Moreover, the correction is order g^1, which is different from previous perturbative computation os entanglement entropy considered in [123][124], where corrections start from the second order. This is because we are using double trace deformation, not single trace deformation.

Let us compare our result with energy of the half space with left end point at (t, x), so the energy is

$$\int_x^\infty d\tilde{x} T_{00}(t, \tilde{x}) \tag{204}$$

. The integral of the energy density is given by

$$\langle \int_x^\infty d\tilde{x} T_{00}(t, \tilde{x}) \rangle = -\frac{4\pi gh}{L^{4h+1}} \Big(\theta(-(x-t)) - \theta(-(x-t-L)) - \theta(-(x+t)) + \theta(-(x+t-L)) \Big). \tag{205}$$

The averaged null energy on null geodesic $(t,\ x) = \lambda, a + \lambda)$ is given by

$$\int_{-\infty}^\infty d\lambda \langle T(t = \lambda, x = a + \lambda) - \tilde{T}(t = \lambda, x = a + \lambda) \rangle = -\frac{4\pi gh}{L^{4h+1}} \theta(L - a)\theta(a). \tag{206}$$

When g is positive, the average null energy is negative, consistent with the calculations in

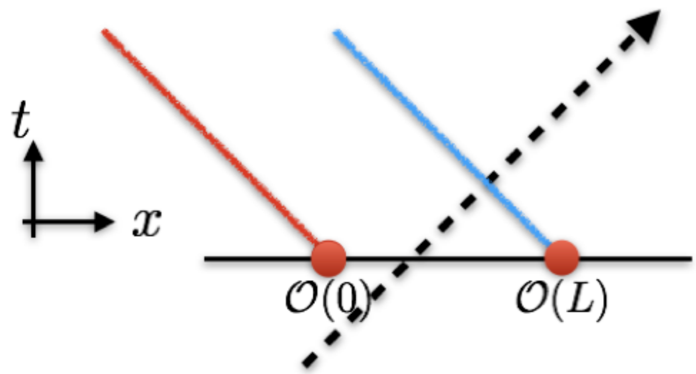

Figure 25: When null geodesic crosses with null blue line, ANE changes by $-\frac{4\pi gh}{L^{4h+1}}$, and $\frac{4\pi gh}{L^{4h+1}}$ with null red line. In particular, when $0 < a < 0$, averaged null energy is $-\frac{4\pi gh}{L^{4h+1}}$, and otherwise zero.

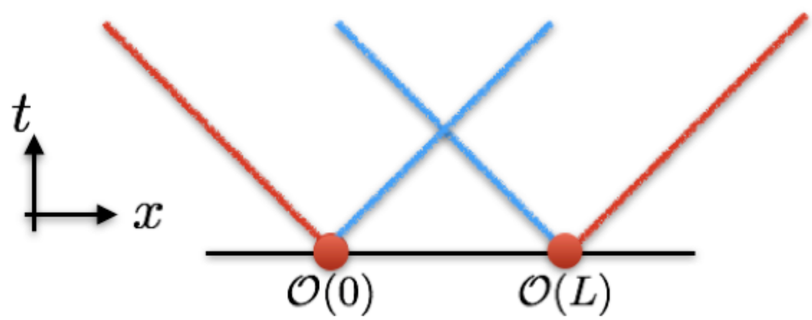

Figure 26: When constant time slice crosses null blue line, the total energy changes by $\frac{4\pi gh}{L^{4h+1}}$, and $-\frac{4\pi gh}{L^{4h+1}}$ with null red line. In particular, the total energy is always 0 after double trace deformation.

the bulk. Further, the perturbation is not UV divergent and is finite. Note that ANE is nonzero only when $0 < a < L$. This is because of cancelation of positive energy flux and negative energy flux. Note that for excited states, the energy always increases. However, for our case, the total energy does not change at leading order since we are considering external instantaneous perturbation.

5.7 Renyi Entanglement Entropy

Next, we consider time evolution of Renyi entropy after acting non local double trace deformation in two dimensional CFT. The shift of n-th Renyi entropy $\Delta S_A^n(g,t) = S_A^n(g,t) - S_A^n(0)$ can be computed using replica trick[112][125],

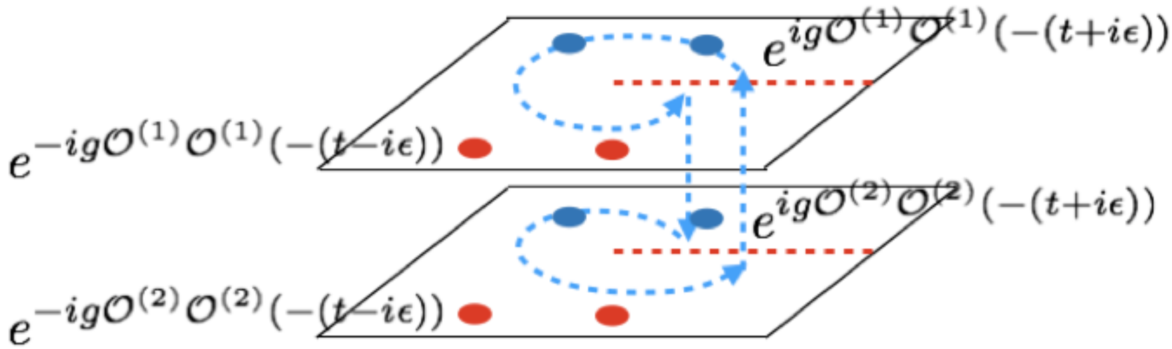

Figure 27: Geometry of replica Σ_2. Blue points correspond to $e^{ig\mathcal{O}\mathcal{O}(-(t+i\epsilon))}$, and red points correspond to $e^{ig\mathcal{O}\mathcal{O}(-(t-i\epsilon))}$.

$$\Delta S_A^n(g,t) = \frac{1}{1-n} log \frac{\langle e^{ig\mathcal{O}^{\dagger(1)}(-(t+i\epsilon),-x)\mathcal{O}^{\dagger(1)}(-(t+i\epsilon),-x+L)} e^{-ig\mathcal{O}^{(1)}(-(t-i\epsilon),-x)\mathcal{O}^{(1)}(-(t-i\epsilon),-x+L)} \cdots \rangle_{\Sigma_n}}{\langle 1 \rangle_{\Sigma_n}}. \tag{207}$$

where Σ_n is n-sheeted geometry, and $\mathcal{O}^{(i)}$ lives on i-th sheet. We assume that the subregion is half line. Then the conformal transformation from Σ_n to Σ_1 is simply given by

$$w = z^n. \tag{208}$$

Let us consider g^1 order contribution,

$$\begin{aligned} &\langle e^{ig\mathcal{O}^{\dagger(1)}\mathcal{O}^{\dagger(1)}(-(t+i\epsilon))} e^{-ig\mathcal{O}^{(1)}\mathcal{O}^{(1)}(-(t-i\epsilon))} \cdots \rangle_{\Sigma_n} \\ &= \langle 1 \rangle_{\Sigma_n} + ig \sum_{i=1}^{n} \left(\langle \mathcal{O}^{(i)\dagger}\mathcal{O}^{(i)\dagger}(-(t+i\epsilon)) \rangle_{\Sigma_n} - \langle \mathcal{O}^{(i)}\mathcal{O}^{(i)}(-(t-i\epsilon)) \rangle_{\Sigma_n} \right) + \mathcal{O}(g^2) \end{aligned} \tag{209}$$

Let us specialize to $n=2$ case. In the first sheet, $w = -x + (t \pm i\epsilon)$ corresponds to

$$z(x,\pm) = \theta(x-t)\sqrt{x-t}e^{\frac{i\pi}{2}} + \theta(t-x)\sqrt{t-x}e^{\frac{i\pi(1\mp 1)}{2}}, \tag{210}$$

and $\bar{z} = -x - (t \pm i\epsilon)$ corresponds to

$$\bar{z}(x,\pm) = \theta(x+t)\sqrt{x+t}e^{\frac{-i\pi}{2}} + \theta(-t-x)\sqrt{-t-x}e^{\frac{-i\pi(1\mp 1)}{2}}. \tag{211}$$

In the second sheet, $w = -x + (t \pm i\epsilon)$ corresponds to

$$z(x,\pm)=\theta(x-t)\sqrt{x-t}e^{\frac{i3\pi}{2}}+\theta(t-x)\sqrt{t-x}e^{\frac{i\pi(3\mp1)}{2}}, \tag{212}$$

and $\bar{z}=-x-(t\pm i\epsilon)$ corresponds to

$$\bar{z}(x,\pm)=\theta(x+t)\sqrt{x+t}e^{\frac{-i3\pi}{2}}+\theta(-t-x)\sqrt{-t-x}e^{\frac{-i\pi(3\mp1)}{2}}. \tag{213}$$

Then we have

$$\begin{aligned}
&\langle\mathcal{O}^{(1)}(-(t\pm i\epsilon),-x)\mathcal{O}^{(1)}(-(t\pm i\epsilon),-x+L)\rangle_{\Sigma_2}\\
&=\langle\mathcal{O}^{(2)}(-(t\pm i\epsilon),-x)\mathcal{O}^{(2)}(-(t\pm i\epsilon),-x+L)\rangle_{\Sigma_2}\\
&=(\frac{dz}{dw})^h|_{z=z(x,\pm)}(\frac{d\bar{z}}{d\bar{w}})^h|_{\bar{z}=\bar{z}(x,\pm)}\\
&\times(\frac{dz}{dw})^h|_{z=z(x-L,\pm)}(\frac{d\bar{z}}{d\bar{w}})^h|_{\bar{z}=\bar{z}(x-L,\pm)}\\
&\langle\mathcal{O}^{(1)}(z(x,\pm),\bar{z}(x,\pm))\mathcal{O}^{(1)}(z(x-L,\pm),\bar{z}(x-L,\pm))\rangle_{\Sigma_1}.
\end{aligned} \tag{214}$$

The results are shown in Figure. We can confirm that the second Renyi entropy behaves in the same way as entanglement entropy. In particular, we have zero Renyi entropy and zero entanglement entropy on identical regions, including regions where any change is prohibited by causality.

5.8 Summary

In this section, we considered non local double trace deformation composed of boundary local operators as well as bulk local operators. We evaluated time shift caused by the deformation, by computing averaged null energy. Then we considered time evolution of CFT, by computing entanglement entropies and Renyi entropies.

In this section, we only computed leading term in g, and entanglement introduced was order c^0. We can consider higher order in g, as well as adding more nonlocal entanglement by $e^{i\sum_l c_l \mathcal{O}_l}$.Generalization of our study to higher order correction might lead to an understanding of constructing wormholes in spacetime with single boundary. Also, it is interesting to apply our bulk local double trace deformation to AdS_2.

In our computation of dynamics of entanglement entropy and entanglement Renyi entropy, we considered instantaneous double trace deformation and leading term which is proportional to g^1. It is interesting and tractable to generalize this computation to higher order, or to triple trace deformations. Triple trace deformation can be an interesting example to examine multi partite entanglement.

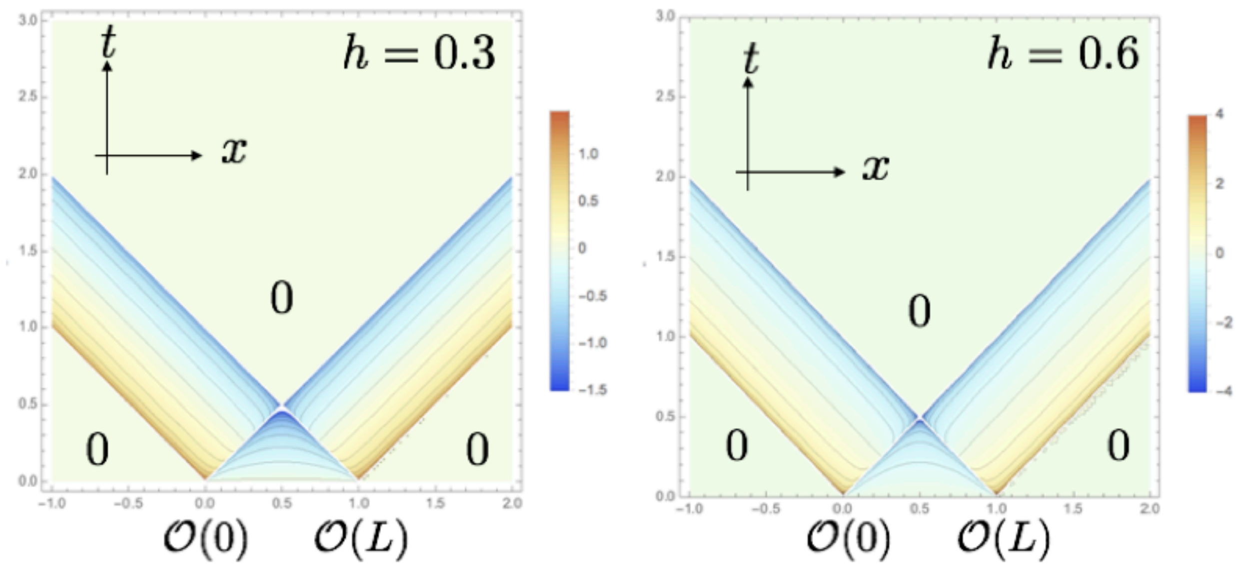

Figure 28: Entanglement Renyi entropy ΔS_A^2 of semi infinite half line divided by coupling g. Value of Renyi entropy depends on the location of the left edge of the half line, which is specified by the coordinate (t, x). When $x > t + L$ or $x + t < 0$, ΔS_A^2 must be zero from causality. Left figure is for $h = 0.3$ and right one is for $h = 0.6$. In all case one can observe that Renyi entropy behaves in similar way as that of entanglement entropy.

6 Conclusion and Future Directions

In this thesis, I first explained basics of AdS/CFT and pure AdS spacetimes, and introduced several bipartite entanglement measures that capture pure quantum bipartite entanglement. Then I reviewed what quantum entanglement plays fundamental role in AdS/CFT.

Then I proposed a holographic dual of a quantum information theoretic measure, called fidelity susceptibility, as the volume of time slice in the bulk which has maximal volume. The proposal is a hard wall approximation of interface CFT with interface probe brane. I compared this proposal in several examples with CFT calculations, including thermofield double state which has highly non trivial time dependence.

Then I proposed an application of fidelity susceptibility to scrambling phenomena, by relating scrambling with sensitivity of dynamics against external perturbation. I showed that distance between states, which are the same initially, with slightly different Hamiltonians will grow exponentially with Lyapunov exponent, diagnosing "butterfly effect". This is because in such case, fidelity susceptibility is proportional to commutators of operators. I also showed that by computing maximal volume in shock wave geometry, holographic fidelity susceptibility grows exponentially in time, as expected.

Finally, I studied dynamics of gravity and CFT after introduction of non local double trace deformation. Such deformation corresponds to quantum channels in quantum information theory. I observed violation of averaged null energy condition, implying enlargement of causal cone. In other words, originally light like geodesic becomes space like after deformation. I also studied how entanglement entropy and Renyi entropy evolves in time.

There are number of interesting research directions related to the studies discussed in this paper. First it is interesting to explore CFT and holographic computations of bipartite entanglement measures, explained in the second section of this thesis. One possible direction to this question is to use tensor networks and optimization, as discussed in [127].

It is also intriguing to explore dynamics of gravity using AdS/CFT. Once we obtained information on CFT up to non-perturbative order in c, one can obtain information on quantum gravity, non-perturbative in G_N. Such direction was discussed in [128]. One interesting extension of section 5 related to this direction is to consider formation of binary black hole from entangled matter. Such configuration is expected to lead to two sided black hole or non-traversable wormhole, but such expectation has never been quantitatively examined.

There is also an interesting direction toward computing fidelity susceptibility directly from AdS/CFT [129][130]. They constructed symplectic form on the manifold of quantum states parametrized by sources, whose Kahler metric for marginal deformation coincides with fidelity susceptibility. They found a bulk expression of fidelity susceptibility given by integral of a form on bulk time slice.

Acknowledgement

I would like to appreciate my advisor Tadashi Takayanagi for collaborations, fruitful discussions and advises. I am grateful to Arpan Bhattacharyya, Pawel Caputa, Nilay Kundu, Tokiro Numasawa, Noburo Shiba, Shinsei Ryu, Kento Watanabe and Xueda Wen for insightful discussions and collaborations. I thank Shinya Aoki, Yuya Kusuki, Masahiro Nozaki, Seiji Terashima, Koji Umemoto, and Aron Wall for useful discussions and correspondences. The author is supported by JSPS fellowship and by JSPS Grant-in-Aid for JSPS Fellows No.16J08909.

References

[1] M. B. Green, J. H. Schwarz and E. Witten, "Superstring Theory. Vol. 1: Introduction," Cambridge, Uk: Univ. Pr. (1987) 469 P. (Cambridge Monographs On Mathematical Physics), "Superstring Theory. Vol. 2: Loop Amplitudes, Anomalies And Phenomenology," Cambridge, Uk: Univ. Pr. (1987) 596 P. (Cambridge Monographs On Mathematical Physics)

[2] J. Polchinski, "String theory. Vol. 1: An introduction to the bosonic string," doi:10.1017/CBO9780511816079, "String theory. Vol. 2: Superstring theory and beyond," doi:10.1017/CBO9780511618123

[3] J. D. Bekenstein, Phys. Rev. D **7**, 2333 (1973). doi:10.1103/PhysRevD.7.2333

[4] S. W. Hawking, "Particle Creation by Black Holes," Commun. Math. Phys. **43**, 199 (1975) Erratum: [Commun. Math. Phys. **46**, 206 (1976)]. doi:10.1007/BF02345020, 10.1007/BF01608497

[5] A. Strominger and C. Vafa, "Microscopic origin of the Bekenstein-Hawking entropy," Phys. Lett. B **379**, 99 (1996) doi:10.1016/0370-2693(96)00345-0 [hep-th/9601029].

[6] G. 't Hooft, "Dimensional reduction in quantum gravity," Conf. Proc. C **930308**, 284 (1993) [gr-qc/9310026].

[7] L. Susskind, "The World as a hologram," J. Math. Phys. **36**, 6377 (1995) doi:10.1063/1.531249 [hep-th/9409089].

[8] X. O. Camanho, J. D. Edelstein, J. Maldacena and A. Zhiboedov, "Causality Constraints on Corrections to the Graviton Three-Point Coupling," JHEP **1602**, 020 (2016) doi:10.1007/JHEP02(2016)020 [arXiv:1407.5597 [hep-th]].

[9] J. M. Maldacena, Int. J. Theor. Phys. **38**, 1113 (1999) [Adv. Theor. Math. Phys. **2**, 231 (1998)] doi:10.1023/A:1026654312961, 10.4310/ATMP.1998.v2.n2.a1 [hep-th/9711200].

[10] S. S. Gubser, I. R. Klebanov and A. M. Polyakov, "Gauge theory correlators from non-critical string theory," Phys. Lett. B **428**, 105 (1998) doi:10.1016/S0370-2693(98)00377-3 [hep-th/9802109].

[11] E. Witten, "Anti-de Sitter space and holography," Adv. Theor. Math. Phys. **2**, 253 (1998) doi:10.4310/ATMP.1998.v2.n2.a2 [hep-th/9802150].

[12] S. Ryu and T. Takayanagi, "Holographic derivation of entanglement entropy from AdS/CFT," Phys. Rev. Lett. **96**, 181602 (2006) doi:10.1103/PhysRevLett.96.181602 [hep-th/0603001].

[13] M. Headrick and T. Takayanagi, "A Holographic proof of the strong subadditivity of entanglement entropy," Phys. Rev. D **76**, 106013 (2007) doi:10.1103/PhysRevD.76.106013 [arXiv:0704.3719 [hep-th]].

[14] A. Lewkowycz and J. Maldacena, "Generalized gravitational entropy," JHEP **1308**, 090 (2013) doi:10.1007/JHEP08(2013)090 [arXiv:1304.4926 [hep-th]].

[15] M. Nozaki, T. Numasawa and T. Takayanagi, "Holographic Local Quenches and Entanglement Density," JHEP **1305**, 080 (2013) doi:10.1007/JHEP05(2013)080 [arXiv:1302.5703 [hep-th]].

[16] M. Nozaki, T. Numasawa, A. Prudenziati and T. Takayanagi, "Dynamics of Entanglement Entropy from Einstein Equation," Phys. Rev. D **88**, no. 2, 026012 (2013) doi:10.1103/PhysRevD.88.026012 [arXiv:1304.7100 [hep-th]].

[17] N. Lashkari, M. B. McDermott and M. Van Raamsdonk, "Gravitational dynamics from entanglement 'thermodynamics'," JHEP **1404**, 195 (2014) doi:10.1007/JHEP04(2014)195 [arXiv:1308.3716 [hep-th]].

[18] T. Faulkner, M. Guica, T. Hartman, R. C. Myers and M. Van Raamsdonk, "Gravitation from Entanglement in Holographic CFTs," JHEP **1403**, 051 (2014) doi:10.1007/JHEP03(2014)051 [arXiv:1312.7856 [hep-th]].

[19] V. E. Hubeny, M. Rangamani and T. Takayanagi, "A Covariant holographic entanglement entropy proposal," JHEP **0707**, 062 (2007) doi:10.1088/1126-6708/2007/07/062 [arXiv:0705.0016 [hep-th]].

[20] M. Van Raamsdonk, "Building up spacetime with quantum entanglement," Gen. Rel. Grav. **42**, 2323 (2010) [Int. J. Mod. Phys. D **19**, 2429 (2010)] doi:10.1007/s10714-010-1034-0, 10.1142/S0218271810018529 [arXiv:1005.3035 [hep-th]].

[21] J. M. Maldacena, "Eternal black holes in anti-de Sitter," JHEP **0304**, 021 (2003) doi:10.1088/1126-6708/2003/04/021 [hep-th/0106112].

[22] A. C. Wall, "Maximin Surfaces, and the Strong Subadditivity of the Covariant Holographic Entanglement Entropy," Class. Quant. Grav. **31**, no. 22, 225007 (2014) doi:10.1088/0264-9381/31/22/225007 [arXiv:1211.3494 [hep-th]].

[23] R. Horodecki, P. Horodecki, M. Horodecki and K. Horodecki, "Quantum entanglement," Rev. Mod. Phys. **81**, 865 (2009) doi:10.1103/RevModPhys.81.865 [quant-ph/0702225].

[24] J. Eisert, M. Cramer and M. B. Plenio, Rev. Mod. Phys. **82**, 277 (2010) doi:10.1103/RevModPhys.82.277 [arXiv:0808.3773 [quant-ph]].

[25] A. Kitaev and J. Preskill, "Topological entanglement entropy," Phys. Rev. Lett. **96**, 110404 (2006) doi:10.1103/PhysRevLett.96.110404 [hep-th/0510092].

[26] M. Levin and X. G. Wen, "Detecting Topological Order in a Ground State Wave Function," Phys. Rev. Lett. **96**, 110405 (2006) doi:10.1103/PhysRevLett.96.110405 [cond-mat/0510613 [cond-mat.str-el]].

[27] R. F. Werner, "Quantum states with Einstein-Podolsky-Rosen correlations admitting a hidden-variable model," Phys. Rev. A **40**, 4277 (1989). doi:10.1103/PhysRevA.40.4277

[28] A. Peres, "Separability criterion for density matrices," Phys. Rev. Lett. **77**, 1413 (1996) doi:10.1103/PhysRevLett.77.1413 [quant-ph/9604005].

[29] M. Miyaji, T. Numasawa, N. Shiba, T. Takayanagi and K. Watanabe, "Distance between Quantum States and Gauge-Gravity Duality," Phys. Rev. Lett. **115**, no. 26, 261602 (2015) doi:10.1103/PhysRevLett.115.261602 [arXiv:1507.07555 [hep-th]].

[30] M. Miyaji, "Butterflies from Information Metric," JHEP **1609**, 002 (2016) doi:10.1007/JHEP09(2016)002 [arXiv:1607.01467 [hep-th]].

[31] M. Miyaji, "Time Evolution after Double Trace Deformation," JHEP **1810**, 074 (2018) doi:10.1007/JHEP10(2018)074 [arXiv:1806.10807 [hep-th]].

[32] P. Calabrese, J. Cardy and E. Tonni, "Entanglement negativity in quantum field theory," Phys. Rev. Lett. **109**, 130502 (2012) doi:10.1103/PhysRevLett.109.130502 [arXiv:1206.3092 [cond-mat.stat-mech]].

[33] J. M. Maldacena, "Eternal black holes in anti-de Sitter," JHEP **0304**, 021 (2003) doi:10.1088/1126-6708/2003/04/021 [hep-th/0106112].

[34] L. Susskind, "Computational Complexity and Black Hole Horizons," [Fortsch. Phys. **64**, 24 (2016)] Addendum: Fortsch. Phys. **64**, 44 (2016) doi:10.1002/prop.201500093, 10.1002/prop.201500092 [arXiv:1403.5695 [hep-th], arXiv:1402.5674 [hep-th]].

[35] D. Stanford and L. Susskind, "Complexity and Shock Wave Geometries," Phys. Rev. D **90**, no. 12, 126007 (2014) doi:10.1103/PhysRevD.90.126007 [arXiv:1406.2678 [hep-th]].

[36] S. L. Braunstein and C. M. Caves, "Statistical distance and the geometry of quantum states," Phys. Rev. Lett. **72**, 3439 (1994). doi:10.1103/PhysRevLett.72.3439

[37] M. Nozaki, S. Ryu and T. Takayanagi, "Holographic Geometry of Entanglement Renormalization in Quantum Field Theories," JHEP **1210**, 193 (2012) doi:10.1007/JHEP10(2012)193 [arXiv:1208.3469 [hep-th]].

[38] S-J. Gu, "Fidelity approach to quantum phase transitions", Int. J. Mod. Phys. B **24** (2010) 4371.

[39] D. Bak, M. Gutperle and S. Hirano, "A Dilatonic deformation of AdS(5) and its field theory dual," JHEP **0305**, 072 (2003) doi:10.1088/1126-6708/2003/05/072 [hep-th/0304129].

[40] D. Bak, M. Gutperle and S. Hirano, "Three dimensional Janus and time-dependent black holes," JHEP **0702**, 068 (2007) doi:10.1088/1126-6708/2007/02/068 [hep-th/0701108].

[41] A. Karch and L. Randall, "Locally localized gravity," JHEP **0105**, 008 (2001) doi:10.1088/1126-6708/2001/05/008 [hep-th/0011156].

[42] T. Azeyanagi, A. Karch, T. Takayanagi and E. G. Thompson, "Holographic calculation of boundary entropy," JHEP **0803**, 054 (2008) doi:10.1088/1126-6708/2008/03/054 [arXiv:0712.1850 [hep-th]].

[43] T. Takayanagi, "Holographic Dual of BCFT," Phys. Rev. Lett. **107**, 101602 (2011) doi:10.1103/PhysRevLett.107.101602 [arXiv:1105.5165 [hep-th]], M. Fujita, T. Takayanagi and E. Tonni, "Aspects of AdS/BCFT," JHEP **1111**, 043 (2011) doi:10.1007/JHEP11(2011)043 [arXiv:1108.5152 [hep-th]].

[44] J. Erlich, E. Katz, D. T. Son and M. A. Stephanov, "QCD and a holographic model of hadrons," Phys. Rev. Lett. **95**, 261602 (2005) doi:10.1103/PhysRevLett.95.261602 [hep-ph/0501128].

[45] M. Nozaki, T. Takayanagi and T. Ugajin, "Central Charges for BCFTs and Holography," JHEP **1206**, 066 (2012) doi:10.1007/JHEP06(2012)066 [arXiv:1205.1573 [hep-th]].

[46] T. Hartman and J. Maldacena, "Time Evolution of Entanglement Entropy from Black Hole Interiors," JHEP **1305**, 014 (2013) doi:10.1007/JHEP05(2013)014 [arXiv:1303.1080 [hep-th]].

[47] P. Hayden and J. Preskill, "Black holes as mirrors: Quantum information in random subsystems," JHEP **0709**, 120 (2007) doi:10.1088/1126-6708/2007/09/120 [arXiv:0708.4025 [hep-th]].

[48] A. Kitaev. "Hidden correlations in the Hawking radiation and thermal noise." - 2014. Talk given at the Fundamental Physics Prize Symposium, Nov. 10.

[49] Y. Sekino and L. Susskind, "Fast Scramblers," JHEP **0810**, 065 (2008) doi:10.1088/1126-6708/2008/10/065 [arXiv:0808.2096 [hep-th]].

[50] S. H. Shenker and D. Stanford, "Black holes and the butterfly effect," JHEP **1403**, 067 (2014) doi:10.1007/JHEP03(2014)067 [arXiv:1306.0622 [hep-th]].

[51] J. Maldacena, S. H. Shenker and D. Stanford, "A bound on chaos," [arXiv:1503.01409 [hep-th]].

[52] A. I. Larkin and Y. N. Ovchinnikov, "Quasiclassical Method in the Theory of Superconductivity", JETP 28, 6 (1969): 1200-1205.

[53] S. H. Shenker and D. Stanford, "Multiple Shocks," JHEP **1412**, 046 (2014) doi:10.1007/JHEP12(2014)046 [arXiv:1312.3296 [hep-th]].

[54] S. H. Shenker and D. Stanford, "Stringy effects in scrambling," JHEP **1505**, 132 (2015) doi:10.1007/JHEP05(2015)132 [arXiv:1412.6087 [hep-th]].

[55] D. A. Roberts, D. Stanford and L. Susskind, “Localized shocks,” JHEP **1503**, 051 (2015) doi:10.1007/JHEP03(2015)051 [arXiv:1409.8180 [hep-th]].

[56] D. A. Roberts and D. Stanford, “Two-dimensional conformal field theory and the butterfly effect,” Phys. Rev. Lett. **115**, no. 13, 131603 (2015) doi:10.1103/PhysRevLett.115.131603 [arXiv:1412.5123 [hep-th]].

[57] P. Caputa, J. Simon, A. Stikonas, T. Takayanagi and K. Watanabe, “Scrambling time from local perturbations of the eternal BTZ black hole,” JHEP **1508**, 011 (2015) doi:10.1007/JHEP08(2015)011 [arXiv:1503.08161 [hep-th]].

[58] A. Kitaev, “A simple model of quantum holography.” http://online.kitp.ucsb.edu/online/entangled15/kitaev/, Talks at KITP, April 7, 2015. http://online.kitp.ucsb.edu/online/entangled15/kitaev2/. Talks at KITP, May 27, 2015.

[59] D. Stanford, “Many-body chaos at weak coupling,” [arXiv:1512.07687 [hep-th]].

[60] B. Michel, J. Polchinski, V. Rosenhaus and S. J. Suh, “Four-point function in the IOP matrix model,” [arXiv:1602.06422 [hep-th]].

[61] P. Caputa, T. Numasawa and A. Veliz-Osorio, “Scrambling without chaos in RCFT,” [arXiv:1602.06542 [hep-th]].

[62] Y. Gu and X. L. Qi, “Fractional Statistics and the Butterfly Effect,” [arXiv:1602.06543 [hep-th]].

[63] A. L. Fitzpatrick and J. Kaplan, “A Quantum Correction To Chaos,” [arXiv:1601.06164 [hep-th]].

[64] H. Chen, A. L. Fitzpatrick, J. Kaplan, D. Li and J. Wang, “Degenerate Operators and the $1/c$ Expansion: Lorentzian Resummations, High Order Computations, and Super-Virasoro Blocks,” [arXiv:1606.02659 [hep-th]].

[65] S. Jackson, L. McGough and H. Verlinde, “Conformal Bootstrap, Universality and Gravitational Scattering,” Nucl. Phys. B **901**, 382 (2015) doi:10.1016/j.nuclphysb.2015.10.013 [arXiv:1412.5205 [hep-th]].

[66] J. Polchinski, “Chaos in the black hole S-matrix,” [arXiv:1505.08108 [hep-th]].

[67] P. Hosur, X. L. Qi, D. A. Roberts and B. Yoshida, “Chaos in quantum channels,” JHEP **1602**, 004 (2016) doi:10.1007/JHEP02(2016)004 [arXiv:1511.04021 [hep-th]].

[68] G. Gur-Ari, M. Hanada and S. H. Shenker, “Chaos in Classical D0-Brane Mechanics,” JHEP **1602**, 091 (2016) doi:10.1007/JHEP02(2016)091 [arXiv:1512.00019 [hep-th]].

[69] E. Berkowitz, M. Hanada and J. Maltz, “Chaos in Matrix Models and Black Hole Evaporation,” [arXiv:1602.01473 [hep-th]].

[70] B. Swingle, G. Bentsen, M. Schleier-Smith and P. Hayden, “Measuring the scrambling of quantum information,” [arXiv:1602.06271 [quant-ph]].

[71] E. Perlmutter, “Bounding the Space of Holographic CFTs with Chaos,” [arXiv:1602.08272 [hep-th]].

[72] N. Sircar, J. Sonnenschein, W. Tangarife, [arXiv:1602.07307 [hep-th]]

[73] A. Peres, Quantum Theory: Concepts and Methods (Kluwer Academic Publishers, Dordrecht, 1995).

[74] R. Jalabert and H. Pastawski Phys. Rev. Lett. 86, 2490 (2001)[cond-mat/0010094]

[75] P. Jacquod, P. Silvestrov, and C. Beenakker Phys. Rev. E 64 (2001)[nlin/0107044]

[76] N. Cerruti and S. Tomsovic Phys. Rev. Lett. 88, 054103(2002)[nlin/0108016]

[77] T. Prosen and M. Znidaric, J. Phys. A 35 (2002) 1455-1481[nlin/0111014]

[78] Z. Karkuszewski, C. Jarzynski and W. Zurek, Phys. Rev. Lett. 89 (2002) 170405 [quant-ph/0111002]

[79] T. Prosen and T.H. Seligman, "A random matrix formulation of fidelity decay", J. Phys. A 35 (2002) 4707-4727[nlin/0311022]

[80] J. Emerson, Y. Weinstein, S. Lloyd, and D. Cory, Phys. Rev. Lett. 89, 284102(2002)[quant-ph/0207099]

[81] T. Gorin, T. Prosen, T. Seligman, and M. Znidaric, Phys. Rep. 435, 33(2006)[quant-ph/0607050]

[82] A. Goussev, R. A. Jalabert, H. M. Pastawski, and D. A. Wisniacki, Scholarpedia 7, 11 687 (2012)[arXiv:1206.6348 [nlin.CD]]

[83] H. P. Breuer, E.-M. Laine and J. Piilo, Phys. Rev. Lett. 103, 210401 (2009) [arXiv:0908.0238 [quant-ph]]

[84] Haikka, P. and Goold, J. and McEndoo, S. and Plastina, F. and Maniscalco, S, Phys. Rev. A, 85, 6, 060101, 4,(2012) [arXiv:1202.2997 [quant-ph]]

[85] H. T. Quan, Z. Song, X. F. Liu, P. Zanardi, and C. P. Sun Phys. Rev. Lett. 96, 140604 (2006)[quant-ph/0509007]

[86] P. Zanardi and N. Paunkovic Phys. Rev. E 74, 031123 (2006) [quant-ph/0512249]

[87] B. Swingle, “Entanglement Renormalization and Holography,” Phys. Rev. D **86**, 065007 (2012) doi:10.1103/PhysRevD.86.065007 [arXiv:0905.1317 [cond-mat.str-el]].

[88] M. Miyaji, S. Ryu, T. Takayanagi and X. Wen, “Boundary States as Holographic Duals of Trivial Spacetimes,” JHEP **1505**, 152 (2015) doi:10.1007/JHEP05(2015)152 [arXiv:1412.6226 [hep-th]], M. Miyaji and T. Takayanagi, “Surface/State Correspondence as a Generalized Holography,” PTEP **2015**, no. 7, 073B03 (2015) doi:10.1093/ptep/ptv089 [arXiv:1503.03542 [hep-th]]

[89] S. J. Rey and J. T. Yee, "Macroscopic strings as heavy quarks in large N gauge theory and anti-de Sitter supergravity," Eur. Phys. J. C **22**, 379 (2001) doi:10.1007/s100520100799 [hep-th/9803001].

[90] J. M. Maldacena, "Wilson loops in large N field theories," Phys. Rev. Lett. **80**, 4859 (1998) doi:10.1103/PhysRevLett.80.4859 [hep-th/9803002].

[91] P. Gao, D. L. Jafferis and A. Wall, "Traversable Wormholes via a Double Trace Deformation," JHEP **1712**, 151 (2017) doi:10.1007/JHEP12(2017)151 [arXiv:1608.05687 [hep-th]].

[92] J. Maldacena, D. Stanford and Z. Yang, "Diving into traversable wormholes," Fortsch. Phys. **65**, no. 5, 1700034 (2017) doi:10.1002/prop.201700034 [arXiv:1704.05333 [hep-th]].

[93] A. Almheiri, A. Mousatov and M. Shyani, "Escaping the Interiors of Pure Boundary-State Black Holes," arXiv:1803.04434 [hep-th].

[94] J. De Boer, S. F. Lokhande, E. Verlinde, R. Van Breukelen and K. Papadodimas, "On the interior geometry of a typical black hole microstate," arXiv:1804.10580 [hep-th].

[95] J. Maldacena and X. L. Qi, "Eternal traversable wormhole," arXiv:1804.00491 [hep-th].

[96] W. R. Kelly and A. C. Wall, "Holographic proof of the averaged null energy condition," Phys. Rev. D **90**, no. 10, 106003 (2014) Erratum: [Phys. Rev. D **91**, no. 6, 069902 (2015)] doi:10.1103/PhysRevD.90.106003, 10.1103/PhysRevD.91.069902 [arXiv:1408.3566 [gr-qc]].

[97] T. Faulkner, R. G. Leigh, O. Parrikar and H. Wang, "Modular Hamiltonians for Deformed Half-Spaces and the Averaged Null Energy Condition," JHEP **1609**, 038 (2016) doi:10.1007/JHEP09(2016)038 [arXiv:1605.08072 [hep-th]].

[98] T. Hartman, S. Kundu and A. Tajdini, "Averaged Null Energy Condition from Causality," JHEP **1707**, 066 (2017) doi:10.1007/JHEP07(2017)066 [arXiv:1610.05308 [hep-th]].

[99] R. Bousso, Z. Fisher, J. Koeller, S. Leichenauer and A. C. Wall, "Proof of the Quantum Null Energy Condition," Phys. Rev. D **93**, no. 2, 024017 (2016) doi:10.1103/PhysRevD.93.024017 [arXiv:1509.02542 [hep-th]].

[100] J. Koeller and S. Leichenauer, "Holographic Proof of the Quantum Null Energy Condition," Phys. Rev. D **94**, no. 2, 024026 (2016) doi:10.1103/PhysRevD.94.024026 [arXiv:1512.06109 [hep-th]].

[101] A. C. Wall, "Lower Bound on the Energy Density in Classical and Quantum Field Theories," Phys. Rev. Lett. **118**, no. 15, 151601 (2017) doi:10.1103/PhysRevLett.118.151601 [arXiv:1701.03196 [hep-th]].

[102] S. Balakrishnan, T. Faulkner, Z. U. Khandker and H. Wang, "A General Proof of the Quantum Null Energy Condition," arXiv:1706.09432 [hep-th].

[103] A. Hamilton, D. N. Kabat, G. Lifschytz and D. A. Lowe, "Holographic representation of local bulk operators," Phys. Rev. D **74**, 066009 (2006) doi:10.1103/PhysRevD.74.066009 [hep-th/0606141].

[104] J. Maldacena, A. Milekhin and F. Popov, "Traversable wormholes in four dimensions," arXiv:1807.04726 [hep-th].

[105] I. Ichinose and Y. Satoh, "Entropies of scalar fields on three-dimensional black holes," Nucl. Phys. B **447**, 340 (1995) doi:10.1016/0550-3213(95)00197-Z [hep-th/9412144].

[106] Shapiro, I. I. Fourth test of general relativity. Phys. Rev. Lett. 13, 789 - 791 (1964).

[107] M. Visser, B. Bassett and S. Liberati, "Superluminal censorship," Nucl. Phys. Proc. Suppl. **88**, 267 (2000) doi:10.1016/S0920-5632(00)00782-9 [gr-qc/9810026].

[108] S. Gao and R. M. Wald, "Theorems on gravitational time delay and related issues," Class. Quant. Grav. **17**, 4999 (2000) doi:10.1088/0264-9381/17/24/305 [gr-qc/0007021].

[109] N. Engelhardt and S. Fischetti, "The Gravity Dual of Boundary Causality," Class. Quant. Grav. **33**, no. 17, 175004 (2016) doi:10.1088/0264-9381/33/17/175004 [arXiv:1604.03944 [hep-th]].

[110] M. Miyaji, T. Numasawa, N. Shiba, T. Takayanagi and K. Watanabe, "Continuous Multiscale Entanglement Renormalization Ansatz as Holographic Surface-State Correspondence," Phys. Rev. Lett. **115**, no. 17, 171602 (2015) doi:10.1103/PhysRevLett.115.171602 [arXiv:1506.01353 [hep-th]].

[111] K. Goto, M. Miyaji and T. Takayanagi, "Causal Evolutions of Bulk Local Excitations from CFT," JHEP **1609**, 130 (2016) doi:10.1007/JHEP09(2016)130 [arXiv:1605.02835 [hep-th]].

[112] P. Calabrese and J. L. Cardy, "Entanglement entropy and quantum field theory," J. Stat. Mech. **0406**, P06002 (2004) doi:10.1088/1742-5468/2004/06/P06002 [hep-th/0405152].

[113] P. Calabrese and J. L. Cardy, "Evolution of entanglement entropy in one-dimensional systems," J. Stat. Mech. **0504**, P04010 (2005) doi:10.1088/1742-5468/2005/04/P04010 [cond-mat/0503393].

[114] P. Calabrese and J. Cardy, "Entanglement and correlation functions following a local quench: a conformal field theory approach," J. Stat. Mech. **0710**, no. 10, P10004 (2007) doi:10.1088/1742-5468/2007/10/P10004 [arXiv:0708.3750 [quant-ph]].

[115] P. Caputa, M. Nozaki and T. Takayanagi, "Entanglement of local operators in large-N conformal field theories," PTEP **2014**, 093B06 (2014) doi:10.1093/ptep/ptu122 [arXiv:1405.5946 [hep-th]].

[116] M. Nozaki, "Notes on Quantum Entanglement of Local Operators," JHEP **1410**, 147 (2014) doi:10.1007/JHEP10(2014)147 [arXiv:1405.5875 [hep-th]].

[117] M. Nozaki, T. Numasawa and T. Takayanagi, "Quantum Entanglement of Local Operators in Conformal Field Theories," Phys. Rev. Lett. **112**, 111602 (2014) doi:10.1103/PhysRevLett.112.111602 [arXiv:1401.0539 [hep-th]].

[118] S. He, T. Numasawa, T. Takayanagi and K. Watanabe, "Quantum dimension as entanglement entropy in two dimensional conformal field theories," Phys. Rev. D **90**, no. 4, 041701 (2014) doi:10.1103/PhysRevD.90.041701 [arXiv:1403.0702 [hep-th]].

[119] S. Leichenauer, M. Moosa and M. Smolkin, "Dynamics of the Area Law of Entanglement Entropy," JHEP **1609**, 035 (2016) doi:10.1007/JHEP09(2016)035 [arXiv:1604.00388 [hep-th]].

[120] N. Shiba and T. Takayanagi, "Volume Law for the Entanglement Entropy in Non-local QFTs," JHEP **1402**, 033 (2014) doi:10.1007/JHEP02(2014)033 [arXiv:1311.1643 [hep-th]].

[121] A. Mollabashi, N. Shiba and T. Takayanagi, "Entanglement between Two Interacting CFTs and Generalized Holographic Entanglement Entropy," JHEP **1404**, 185 (2014) doi:10.1007/JHEP04(2014)185 [arXiv:1403.1393 [hep-th]].

[122] J. J. Bisognano and E. H. Wichmann, "On the Duality Condition for Quantum Fields," J. Math. Phys. **17**, 303 (1976). doi:10.1063/1.522898

[123] V. Rosenhaus and M. Smolkin, "Entanglement Entropy: A Perturbative Calculation," JHEP **1412**, 179 (2014) doi:10.1007/JHEP12(2014)179 [arXiv:1403.3733 [hep-th]].

[124] V. Rosenhaus and M. Smolkin, "Entanglement Entropy for Relevant and Geometric Perturbations," JHEP **1502**, 015 (2015) doi:10.1007/JHEP02(2015)015 [arXiv:1410.6530 [hep-th]].

[125] C. G. Callan, Jr. and F. Wilczek, "On geometric entropy," Phys. Lett. B **333**, 55 (1994) doi:10.1016/0370-2693(94)91007-3 [hep-th/9401072].

[126] Nielsen N A and Chuang I L 2000 Quantum Computation and Information (Cambridge: Cambridge University Press)

[127] P. Caputa, M. Miyaji, T. Takayanagi and K. Umemoto, "Holographic Entanglement of Purification from Conformal Field Theories," arXiv:1812.05268 [hep-th].

[128] H. Chen, C. Hussong, J. Kaplan and D. Li, "A Numerical Approach to Virasoro Blocks and the Information Paradox," JHEP **1709**, 102 (2017) doi:10.1007/JHEP09(2017)102 [arXiv:1703.09727 [hep-th]].

[129] A. Belin, A. Lewkowycz and G. S á rosi, "The boundary dual of the bulk symplectic form," Phys. Lett. B **789**, 71 (2019) doi:10.1016/j.physletb.2018.10.071 [arXiv:1806.10144 [hep-th]].

[130] A. Belin, A. Lewkowycz and G. S á rosi, "Complexity and the bulk volume, a new York time story," arXiv:1811.03097 [hep-th].